Poisson Cluster Process Based Analysis of HetNets with Correlated User and Base Station Locations

Mehrnaz Afshang and Harpreet S. Dhillon

arXiv:1612.07285v1 [cs.IT] 21 Dec 2016

Abstract

This paper develops a comprehensive new approach to the modeling and analysis of heterogeneous cellular networks (HetNets) that accurately incorporates correlation in the locations of users and base stations, which exists due to the deployment of small cell base stations (SBSs) at the places of high user density (termed *user hotspots* in this paper). Modeling the locations of the geographical centers of user hotspots as a homogeneous Poisson Point Process (PPP), we assume that the users and SBSs are clustered around each *user hotspot center* independently with two different distributions. The macrocell base station (BS) locations are modeled by an independent PPP. This model naturally captures correlation that exists between the locations of users and their serving SBSs. Using this model, we study the performance of a typical user in terms of coverage probability and *throughput* for two association policies: i) *power-based association*, where a typical user is served by (equivalently, associates with) the open-access BS that provides maximum averaged received power, and ii) *distance-based association*, where a typical user is served by its nearest open-access SBS if it is located closer than a certain *distance threshold*; and macro tier otherwise. After deriving all the results in terms of general distributions describing the locations of users and SBSs around the geographical center of user hotspots, we specialize the setup to the Thomas cluster process, where users and SBSs are clustered with two independent normal distributions. A key intermediate step in this analysis is the derivation of distance distributions from a typical user to the open-access and closed-access interfering SBSs. Consistent with the intuition, our analysis demonstrates that as the number of SBSs reusing the same resource block increases (higher frequency reuse), coverage probability decreases whereas *throughput* increases. Thus the same resource block can be aggressively reused by more SBSs as long as the coverage probability remains acceptable.

Index Terms

Stochastic geometry, Poisson cluster process, user-centric capacity-driven deployment.

The authors are with Wireless@VT, Department of ECE, Virgina Tech, Blacksburg, VA, USA. Email: {mehrnaz, hdhillon}@vt.edu. The support of the US NSF (Grant CCF-1464293 and CNS-1617896) is gratefully acknowledged. This paper will be presented in part at the IEEE WCNC conference [1]. Last updated: December 22, 2016.

I. Introduction

Current cellular networks are undergoing a significant transformation from coverage-driven deployment of macrocells to a more user-centric capacity-driven deployment of several types of low-power BSs, collectively called small cells, usually at the locations of high user density (termed *user hotspots* in this paper) [2], [3]. The resulting network architecture consisting of one or more small cell tiers overlaid on the macrocellular tier is referred to as a HetNet [4]–[7]. The increasing irregularity in the BS locations has led to an increased interest in the use of random spatial models along with tools from stochastic geometry and point process theory for their accurate modeling and tractable analysis; see [8]–[11] for detailed surveys on this topic. The most popular approach in this line of work is to model the locations of different classes of BSs as independent PPPs and perform analysis for a typical user assumed to be located independently of the BS locations. This model was first proposed in [12], [13] for downlink analysis of HetNets, and has been extended to many scenarios of interest in the literature, see [8]–[10] and the references therein. Despite the success of this approach for the modeling and analysis of coverage-centric deployments and conventional single tier macrocellular network [14], this is not quite accurate for modeling user-centric deployments, where the SBSs may be deployed at the user hotspots [2]. In such cases, it is important to accurately capture the non-uniformity of user distributions as well as their correlation with the SBS locations. Developing a comprehensive framework to facilitate the analysis of such setups is the main focus of this paper.

A. Related Work

The stochastic geometry-based modeling and analysis of HetNets has taken two main directions in the literature. The first and more popular one is to focus on the *coverage-centric* analysis of HetNets, in which the user locations are assumed to be independent of the BS locations [8]–[11], [15]. As noted above already, the locations of the different classes of BSs are modeled as independent PPPs. This approach has been extensively used for the analysis of key performance metrics such as coverage/outage probability [12], [16]–[22], rate coverage [23]–[26], average rate [27], and network throughput [28]. In addition, this approach enables the analytic treatment of numerous different aspects of both conventional single-tier networks as well as HetNets. For example, self-powered HetNets where SBSs are powered by a self-contained energy harvesting module were modeled and analyzed in [29]. The downlink coverage and error probability analyses of multiple input multiple output (MIMO) HetNets, where BSs are equipped with multiple

antennas were performed in [25], [30]–[33]. The joint-transmission cooperation in HetNets was analyzed in [19]–[21], [34]. Since this line of work is fairly well-known by now, we refer the interested readers to [8]–[11] for more extensive surveys as well as a more pedagogical treatment of this general research direction.

The second direction focuses on developing tractable models to study user-centric capacity-driven small cell deployments, where SBSs are deployed at the areas of high user density. Due to the technical challenges involved in incorporating this correlation in the BS and user locations, the contributions in this direction are much sparser than above. One key exception is the generative model proposed in [35], where the BS point process is *conditionally thinned* in order to push the reference user closer to its serving BS, thus introducing correlation in the locations of BSs and users. While this model captures the clustering nature of users in hotspots area, it is restricted to single-tier networks and generalization to HetNets is not straightforward. Building on our recent contributions in developing analytical tools for Poisson cluster process (and Binomial point process) [36]–[39], we recently addressed this shortcoming and generalized the analysis of non-uniform user distribution to HetNets by modeling the locations of users as a Poisson cluster process, where the correlation between user and BS locations is captured by placing BSs at the cluster centers [40], [41][1]. Although the models proposed in [35], [40]–[43] accurately characterize the correlation between the user and BS locations, the assumption of modeling small cell locations with a PPP is not quite accurate in the case of user-centric deployments. This is because some user hotspots are by nature large, which necessitates the need to deploy multiple SBSs to cover that area, thus introducing *clustering* in their locations. Similarly, subscriber-owned SBSs, such as femtocells, are deployed on the scale of one per household/business, which naturally increases their density within residential and commercial complexes. Due to this *clustering*, Poisson cluster process becomes preferred choice for modeling SBS locations in user hotspots [44], [45]. While the effect of BS clustering has been studied in [46]–[53], none of these works provide *exact* analytic characterization of interference and key performance metrics for these networks. More importantly, the correlation between user and BS locations, which is the key in user-centric capacity-driven deployments, has not been truly captured in these works. For instance, the locations of users are assumed to be independent of BS point process in [47]. On the other extreme, the users are assumed to be located at a fixed distance from its serving

[1] The analytical tools developed in [36]–[38] are also being adopted to analyze the performance of clustered networks in the emerging paradigms in cellular communication, such as the uplink non-orthogonal multiple access [42].

BS in [51]–[53]. In this paper, we address this shortcoming by developing a new model for user-centric capacity-driven deployments that is realistic as well as tractable. The ability of the proposed analytical model to incorporate correlations in the locations of users and BSs bridges the gap between the spatial models used by the industry (especially for user hotspots), e.g., 3GPP [2], in their simulators, and the ones used by the stochastic geometry community (see above for the detailed discussion) for the performance analysis of HetNets. As discussed next, the main novelty is the use of Poisson cluster process for modeling both the users and the SBSs.

B. Contributions and Outcomes

Tractable model for user-centric capacity-driven deployment of HetNets: We develop a realistic analytic framework to study the performance of user-centric small cell deployments. In particular, we consider a two-tier HetNet, comprising of a tier of small cells overlaid on a macro tier, where macro BSs are distributed as an independent PPP. To capture the dependency between the locations of SBSs and users, we model the geographical centers of user hotspots as an independent PPP around which the SBSs and users form clusters with two independent general distributions. In this setup, the candidate serving BS in each open-access tier is the one that is nearest to the typical user. From the set of candidate serving BSs, the serving BS is chosen based on two association policies: i) *power-based association policy*, where the serving BS is the one that provides the maximum average received power to the typical user, and ii) *distance-based association policy*, where the typical user is served by its nearest open-access SBS if it lies closer than a certain distance threshold; and macro BS otherwise.

Coverage probability and throughput analysis: We derive *exact* expressions for coverage probability of a typical user and throughput of the whole network under the two association policies described above. A key intermediate step in the analysis is the derivation of distance distributions from the typical user to its serving BS, open-access interfering SBSs, and closed-access interfering SBSs for the two association policies. Building on the tools developed for PCPs in [36], we prove that the distances from open-access interfering SBSs conditioned on the location of the serving BS and the typical user are independently and identically distributed (i.i.d.). Using this i.i.d. property, the Laplace transform of interference distribution is obtained, which then enables the derivation of the coverage probability and throughput results.

System design insights: Our analysis leads to several useful design insights for user-centric small cell deployments. First, it reveals that more aggressive frequency reuse within a given

cluster (more SBSs reusing the same resource blocks in a given cluster) has a conflicting effect on the coverage and throughput: throughput increases and coverage decreases. This observation shows that more SBSs can reuse the same resource blocks as long as the coverage probability is acceptable. Thus, the strictly orthogonal resource allocation strategy that allocates each resource block to at most one SBS in a given cluster (e.g., see [47]) may not be efficient in terms of throughput for this setup. Second, our analysis reveals that there exists optimal distance threshold that maximizes the coverage probability of a typical user under distance-based association policy.

II. System Model

We consider a two-tier heterogeneous cellular network consisting of macrocell and small cell BSs, where SBSs and users are clustered around geographical centers of user hotspots, as shown in Fig. 1(c). This model is inspired by the fact that several SBSs may be required to be deployed in the user hotspots (hereafter referred to as cluster) in order to handle mobile data traffic generated in that user hotspot [2]. The analysis is performed for a typical user, which is chosen as follows. We first choose a cluster uniformly at random from the network, which we term a *representative cluster*. We then choose a point (location of the typical user) uniformly at random from this cluster. For this setup, we assume that the typical user is allowed to connect to any macro BS in the whole network and any SBS located within the representative cluster. Other SBSs (the ones located outside the representative cluster) simply act as interferers for the typical user. This setup is inspired by the situations in which SBSs are enterprise owned BSs intended to serve only the authorized users (who have permission to connect to that network). Therefore, we will refer to the macro BSs and the SBSs within the representative cluster as *open access* BSs (with respect to the typical user) and the rest of the SBSs as *closed access* BSs. Note that while our model is, in principle, extendible to completely open access K-tier heterogeneous cellular networks, we limit our discussion to this two-tier setup for the simplicity of both notation and exposition.

A. Spatial Setup and Key Assumptions

We model the locations of macro BSs as an independent homogeneous PPP $\{\mathbf{z}_{\mathrm{m}}\} \equiv \Phi_{\mathrm{m}}$ with destiny λ_{m}. In order to capture the correlation between the locations of SBSs and users in hotspots, we model the locations of SBSs and users as two Poisson cluster processes with the same parent point process, where the later models the geographical centers of user hotspots.

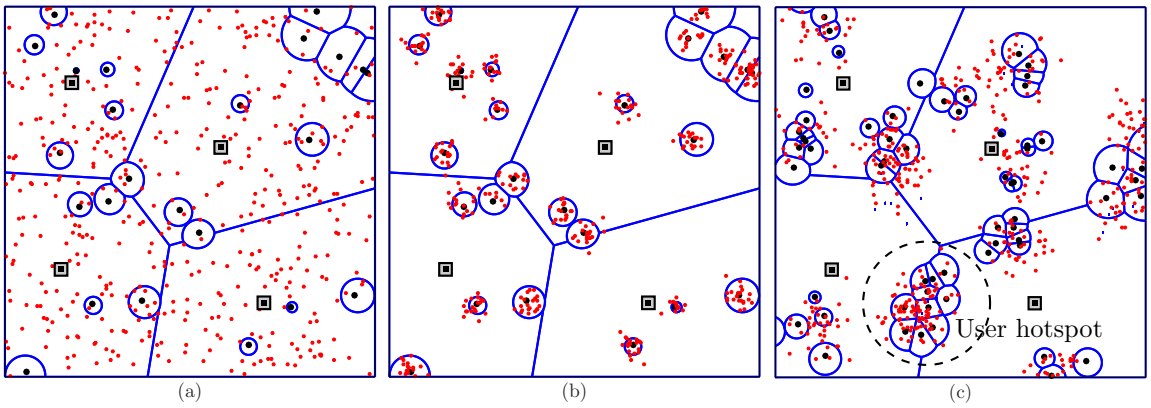

Fig. 1. (a) Coverage-centric deployments where users are uniformly and independently distributed (our original K-tier HetNet model [12]), (b) user-centric deployment where users are clustered around SBSs (recent enhancement to the K-tier model [41]), and (c) user-centric deployment where users and SBSs are clustered around geographical centers of user hotspots (this paper). Black squares, black dots, and small red dots denote the locations of macro BSs, SBSs, and users, respectively.

It should be noted that in reality user distribution is a superposition of homogeneous and non-homogeneous distributions. For instance, pedestrians and users in transit are more likely to be uniformly distributed in the network and hence homogeneous PPP is perhaps a better choice for the analysis of such users. On the other hand, users in hotspots exhibit clustering behavior for which Poisson cluster process is a more appropriate model than a homogeneous PPP [41]. The framework provided in this paper can be extended to the case of mixed user distribution consisting of both homogeneous and non-homogeneous user distributions without much effort. Besides, the analysis of homogeneous user distributions in such setups is well known [8]–[10], [12] , which is the reason we chose to focus on the more challenging case of *correlated* non-homogeneous user distributions.

Poisson cluster process can be formally defined as a union of offspring points which are independent of each other, and identically distributed around parent points [54], [55]. Modeling the locations of parent point process (i.e., cluster centers) as a homogeneous PPP $\{\mathbf{x}\} \equiv \Psi_{\mathrm{p}}$ with density λ_{p},

1) the set of users within a cluster centered at $\mathbf{x} \in \Psi_{\mathrm{p}}$ is denoted by $\{\mathbf{y}_{\mathrm{u}}\} \equiv \mathcal{N}_{\mathrm{u}}^{\mathbf{x}}$ (with $\mathbf{y}_{\mathrm{u}} \in \mathbb{R}^2$), where each set contains a sequence of i.i.d. elements conditional on $\mathbf{x}$ (denoting locations), and the PDF of each element is $f_{\mathbf{Y}_{\mathrm{u}}}(\mathbf{y}_{\mathrm{u}})$, and
2) the set of SBSs within a cluster centered at $\mathbf{x} \in \Psi_{\mathrm{p}}$ is denoted by $\{\mathbf{y}_{\mathrm{s}}\} \equiv \mathcal{N}_{\mathrm{s}}^{\mathbf{x}}$ (with $\mathbf{y}_{\mathrm{s}} \in \mathbb{R}^2$), where each set contains a sequence of i.i.d. elements conditional on $\mathbf{x}$, and the PDF of each element is $f_{\mathbf{Y}_{\mathrm{s}}}(\mathbf{y}_{\mathrm{s}})$.

The locations of SBSs $\mathcal{N}_{\rm s}^{\mathbf{x}}$ and users $\mathcal{N}_{\rm u}^{\mathbf{x}}$ conditioned on $\mathbf{x} \in \Psi_{\rm p}$ are independent. For this setup, after characterizing all theoretical results in terms of general distributions $f_{\mathbf{Y}_{\rm s}}(\mathbf{y}_{\rm s})$ and $f_{\mathbf{Y}_{\rm u}}(\mathbf{y}_{\rm u})$, we specialize the results to Thomas cluster process [56] in which the points are distributed around cluster centers according to an independent Gaussian distribution:

$$f_{\mathbf{Y}_\ell}(\mathbf{y}_\ell) = \frac{1}{2\pi\sigma_\ell^2} \exp\left(-\frac{\|\mathbf{y}_\ell\|^2}{2\sigma_\ell^2}\right), \text{ where } \ell \in \{\mathrm{s}, \mathrm{u}\}, \tag{1}$$

From the set of SBSs located in the cluster centered at $\mathbf{x} \in \Psi_{\rm p}$, we assume that the subset of $\mathcal{B}_{\rm s}^{\mathbf{x}} \subset \mathcal{N}_{\rm s}^{\mathbf{x}}$ reuse the same resource block. This subset will be henceforth referred to as a *set of simultaneously active SBSs*, where the number of simultaneously active SBSs $|\mathcal{B}_{\rm s}^{\mathbf{x}}|$ has a Poisson distribution with mean $\bar{n}_{\rm as}$. Denote by $\mathbf{x}_0 \in \Psi_{\rm p}$ the location of the center of representative cluster. In order to simplify the *order statistics* arguments that will be used in the selection of candidate serving BSs in the cluster located at $\mathbf{x} \in \Psi_p$, we assume that the total number of SBSs (i.e., $|\mathcal{N}_{\rm s}^{\mathbf{x}_0}|$) in the representative cluster is fixed and equal to $n_{\rm s_0}$, where $\mathcal{B}_{\rm s}^{\mathbf{x}_0} \subset \mathcal{N}_{\rm s}^{\mathbf{x}_0}$ represents the set of simultaneously active SBSs in the representative cluster. Note that $|\mathcal{B}_{\rm s}^{\mathbf{x}_0}|$ is truncated Poisson random variable with maximum value being n_{s_0}, and the serving SBS will be chosen from $\mathcal{B}_{\rm s}^{\mathbf{x}_0}$. The pictorial representation of our setup along with the system models used in the prior art are presented in Fig. 1.

B. Propagation Model

We assume that all links to the typical user suffer from a standard power-law path-loss with exponent $\alpha > 2$, and Rayleigh fading. Thus the received power at the typical user (located at the origin) from the j^{th} tier BS (where $j \in \{\mathrm{s}, \mathrm{m}\}$) located at $\mathbf{z}_j$ is:

$$P_{\rm r} = P_j h_j \|\mathbf{z}_j\|^{-\alpha}; \quad j \in \{\mathrm{s}, \mathrm{m}\}, \tag{2}$$

where $\|\cdot\|^{-\alpha}$ models power-law path-loss, h_j is exponential random variable with unit mean independent of all other random variables, and P_j is transmit power, which is assumed to be constant for the BSs in tier $j \in \{\mathrm{s}, \mathrm{m}\}$. Note that index 'm' and 's' refer to macro tier and small cell tier, respectively. Denote by $\{\mathbf{z}_{\rm s} = \mathbf{x}_0 + \mathbf{y}_{\rm s}; \mathbf{y}_{\rm s} \in \mathcal{N}_{\rm s}^{\mathbf{x}_0}\} \equiv \Phi_{\rm s}$ the locations of open-access SBSs. The candidate serving BS location from Φ_j is:

$$\mathbf{z}_j^* = \arg\, \max_{\mathbf{z}_j \in \Phi_j} P_j \|\mathbf{z}_j\|^{-\alpha}, \tag{3}$$

where $\mathbf{z}_j^*$ is the location of the nearest open-access BS of the j^{th} tier (i.e., Φ_j) to the typical user. The serving BS is chosen from amongst the set of candidate serving BSs based on i)

TABLE I
SUMMARY OF NOTATION

Notation	Description
$\Phi_{\mathrm{m}};\ \lambda_{\mathrm{m}}$	Independent PPP modeling the locations of macro BSs; density of Φ_{m}
$\Psi_{\mathrm{p}};\ \lambda_{\mathrm{p}}$	Independent PPP modeling the locations of parent points (cluster centers); density of Ψ_{p}
$\mathcal{N}_{\mathrm{s}}^{\mathbf{x}};\ \mathcal{N}_{\mathrm{u}}^{\mathbf{x}}$	Set of SBSs in cluster centered at $\mathbf{x} \in \Psi_{\mathrm{p}}$; Set of users in cluster centered at $\mathbf{x} \in \Psi_{\mathrm{p}}$
$\mathcal{B}_{\mathrm{s}}^{\mathbf{x}} \subset \mathcal{N}_{\mathrm{s}}^{\mathbf{x}}; \bar{n}_{\mathrm{as}}$	Set of simultaneously active SBSs in cluster centered at $\mathbf{x} \in \Psi_{\mathrm{p}}$ with mean $\bar{n}_{\mathrm{as}}$
$\sigma_{\mathrm{s}}^2\ (\sigma_{\mathrm{u}}^2)$	Scattering variance of the SBS (user) locations around each cluster center
$P_j;\ h_j;\ \alpha;\ \beta$	Transmit power; channel power gain under Rayleigh fading; path loss exponent; target SIR
$\mathcal{A}_j^{\mathrm{P}}\ (\mathcal{A}_j^{\mathrm{D}})$	Association probability under power-based (distance-based) association policy, where $j \in \{\mathrm{s}, \mathrm{m}\}$
$\mathtt{P}_{\mathrm{c}_j}^{\mathrm{P}}\ (\mathtt{P}_{\mathrm{c}_j}^{\mathrm{D}})$	Coverage probability of a typical user served by tier $j \in \{\mathrm{s}, \mathrm{m}\}$ under power-based (distance-based) association policy
$\mathtt{P}_{\mathrm{c_T}}^{\mathrm{P}}\ (\mathtt{P}_{\mathrm{c_T}}^{\mathrm{D}})$	Total coverage probability under power-based (distance-based) association policy
$\mathcal{T}^{\mathrm{P}}\ (\mathcal{T}^{\mathrm{D}})$	Throughput under power-based (distance-based) association policy

power-based, and ii) distance-based association policies. More details on these two association policies will be provided in the next Section.

1) SIR *at a typical user served by macrocell:* Assuming that the typical user is served by the macro BS located at $\mathbf{z}^*$, the total interference seen at the typical user originates from three sources: (i) interference caused by open-access macro BSs (except the serving BS) defined as: $\mathcal{I}_{\mathrm{mm}} = \sum_{\mathbf{z}_{\mathrm{m}} \in \Phi_{\mathrm{m}} \setminus \mathbf{z}^*} P_{\mathrm{m}} h_{\mathrm{m}} \|\mathbf{z}_{\mathrm{m}}\|^{-\alpha}$, (ii) intra-cluster interference caused by simultaneously active open-access SBSs inside the representative cluster, which is defined as: $\mathcal{I}_{\mathrm{sm}}^{\mathrm{intra}} = \sum_{\mathbf{y}_{\mathrm{s}} \in \mathcal{B}_{\mathrm{s}}^{\mathbf{x}_0}} P_{\mathrm{s}} h_{\mathrm{s}} \|\mathbf{x}_0 + \mathbf{y}_{\mathrm{s}}\|^{-\alpha}$, and (iii) inter-cluster interference caused by simultaneously active closed-access SBSs outside the representative cluster, which is defined as: $\mathcal{I}_{\mathrm{sm}}^{\mathrm{inter}} = \sum_{\mathbf{x} \in \Psi_{\mathrm{p}} \setminus \mathbf{x}_0} \sum_{\mathbf{y}_{\mathrm{s}} \in \mathcal{B}_{\mathrm{s}}^{\mathbf{x}}} P_{\mathrm{s}} h_{\mathrm{s}} \|\mathbf{x} + \mathbf{y}_{\mathrm{s}}\|^{-\alpha}$. The SIR at the typical user conditioned on the serving BS being macrocell is:

$$\mathtt{SIR}_{\mathrm{m}} = \frac{P_{\mathrm{m}} h_{\mathrm{m}} \|\mathbf{z}^*\|^{-\alpha}}{\mathcal{I}_{\mathrm{mm}} + \mathcal{I}_{\mathrm{sm}}^{\mathrm{intra}} + \mathcal{I}_{\mathrm{sm}}^{\mathrm{inter}}}. \tag{4}$$

2) SIR *at a typical user served by small cell:* Assuming that a typical user is served by the SBS located at $\mathbf{z}^* = \mathbf{x}_0 + \mathbf{y}_0$, the contribution of the total interference seen at the typical user can be partitioned into three sources: (i) interference from open-access macro BSs defined as: $\mathcal{I}_{\mathrm{ms}} = \sum_{\mathbf{z}_{\mathrm{m}} \in \Phi_{\mathrm{m}}} P_{\mathrm{m}} h_{\mathrm{m}} \|\mathbf{z}_{\mathrm{m}}\|^{-\alpha}$, (ii) interference from simultaneously active open-access SBSs (except the serving BS) inside the representative cluster defined as: $\mathcal{I}_{\mathrm{ss}}^{\mathrm{intra}} = \sum_{\mathbf{y}_{\mathrm{s}} \in \mathcal{B}_{\mathrm{s}}^{\mathbf{x}_0} \setminus \mathbf{y}_0} P_{\mathrm{s}} a_{\mathrm{s}} h_{\mathrm{s}} \|\mathbf{x}_0 + \mathbf{y}_{\mathrm{s}}\|^{-\alpha}$, and (iii) interference from simultaneously active closed-access SBSs outside the representative cluster defined as: $\mathcal{I}_{\mathrm{ss}}^{\mathrm{inter}} = \sum_{\mathbf{x} \in \Psi_{\mathrm{p}} \setminus \mathbf{x}_0} \sum_{\mathbf{y}_{\mathrm{s}} \in \mathcal{B}_{\mathrm{s}}^{\mathbf{x}}} P_{\mathrm{s}} h_{\mathrm{s}} \|\mathbf{x} + \mathbf{y}_{\mathrm{s}}\|^{-\alpha}$. Therefore, the SIR at the typical user served by the small cell is:

$$\mathtt{SIR}_{\mathrm{s}} = \frac{P_{\mathrm{s}} h_{\mathrm{s}} \|\mathbf{z}^*\|^{-\alpha}}{\mathcal{I}_{\mathrm{ms}} + \mathcal{I}_{\mathrm{ss}}^{\mathrm{intra}} + \mathcal{I}_{\mathrm{ss}}^{\mathrm{inter}}}. \tag{5}$$

III. Serving and Interfering Distances

This is the first main technical section of the paper, where we derive the association probability of a typical user to macro BSs and SBSs. We then characterize the distributions of distances from serving and interfering macro BSs and SBSs to a typical user. These distance distributions will be used to characterize the coverage probability of a typical user, and throughput of the whole network in the next section. We now begin by providing relevant distance distributions.

A. Relevant distance distributions

Let us denote the distances from a typical user to its nearest open-access small cell and macro BSs by R_{s} and R_{m}, respectively. In order to calculate the association probability and the serving distance distribution, it is important to first characterize the density functions of R_{m} and R_{s}. The PDF and CDF of the distance from a typical user to its nearest macro BS, i.e., R_{m}, can be easily obtained by using null probability of a homogeneous PPP as [57]:

$$\text{PDF:}\quad f_{R_{\mathrm{m}}}(r_{\mathrm{m}}) = 2\pi\lambda_{\mathrm{m}} r_{\mathrm{m}} \exp(-\pi\lambda_{\mathrm{m}} r_{\mathrm{m}}^2) \qquad \text{CDF:}\quad F_{R_{\mathrm{m}}}(r_{\mathrm{m}}) = 1-\exp(-\pi\lambda_{\mathrm{m}} r_{\mathrm{m}}^2). \tag{6}$$

However, characterizing the density function of distance from a typical user to its nearest open-access SBS, i.e., the nearest SBS to the typical user from representative cluster, is more challenging. To derive the density function of R_{s}, it is useful to define the sequence of distances from the typical user to the SBSs located within the representative cluster as $\mathcal{D}_{\mathrm{s}}^{\mathbf{x}_0} = \{u : u = \|\mathbf{x}_0 + \mathbf{y}_{\mathrm{s}}\|, \forall \mathbf{y}_{\mathrm{s}} \in \mathcal{N}_{\mathrm{s}}^{\mathbf{x}_0}\}$. Note that the elements in $\mathcal{D}_{\mathrm{s}}^{\mathbf{x}_0}$ are correlated due to the common factor $\mathbf{x}_0$. But this correlation can be handled by conditioning on the location of representative cluster center $\mathbf{x}_0$ because the SBS locations are i.i.d. around the cluster center by assumption. The conditional PDF of any (arbitrary) element in the set $\mathcal{D}_{\mathrm{s}}^{\mathbf{x}_0}$ is characterized next.

Lemma 1. *The distances in the set $\mathcal{D}_{\mathrm{s}}^{\mathbf{x}_0}$ conditioned on the distance of the typical user to the cluster center, i.e., $V_0 = \|\mathbf{x}_0\|$, are i.i.d., where the CDF of each element for a given $V_0 = \nu_0$ is:*

$$F_U(u|\nu_0) = \int_{z_1=-u}^{z_1=u} \int_{z_2=-\sqrt{u^2-z_1^2}}^{z_2=\sqrt{u^2-z_1^2}} f_{\mathbf{Y}_{\mathrm{s}}}(z_1-\nu_0, z_2)\mathrm{d}z_2\mathrm{d}z_1, \tag{7}$$

and the conditional PDF of U is:

$$f_U(u|\nu_0) = \int_{-u}^{u} \frac{u}{\sqrt{u^2-z_1^2}} \Big[f_{\mathbf{Y}_{\mathrm{s}}}\Big(z_1-\nu_0, \sqrt{u^2-z_1^2}\Big) + f_{\mathbf{Y}_{\mathrm{s}}}\Big(z_1-\nu_0, -\sqrt{u^2-z_1^2}\Big)\Big]\mathrm{d}z_1, \tag{8}$$

where the PDF of V_0 is given by

$$f_{V_0}(\nu_0) = \int_{-\nu_0}^{\nu_0} \frac{\nu_0}{\sqrt{\nu_0^2-x_1^2}} \Big[f_{\mathbf{Y}_{\mathrm{u}}}\Big(x_1, \sqrt{v_0^2-x_1^2}\Big) + f_{\mathbf{Y}_{\mathrm{u}}}\Big(x_1, -\sqrt{v_0^2-x_1^2}\Big)\Big]\mathrm{d}x_1. \tag{9}$$

Proof: See Appendix A. ■

The density functions of distances presented in Lemma 1 are specialized to the case of Thomas cluster process in the next Corollary.

Corollary 1. *For the special case of Thomas cluster process, the distances in the set $\mathcal{D}_{\mathrm{s}}^{\mathbf{x}_0}$ are conditionally i.i.d., with CDF*

$$F_U(u|\nu_0) = 1 - Q_1\Big(\frac{\nu_0}{\sigma_{\mathrm{s}}}, \frac{u}{\sigma_{\mathrm{s}}}\Big), \quad u > 0, \tag{10}$$

where $Q_1(a,b)$ is the Marcum Q-function defined as $Q_1(a,b) = \int_b^\infty te^{-\frac{t^2+a^2}{2}} I_0(at)\mathrm{d}t$, and the PDF of each element is:

$$f_U(u|\nu_0) = \frac{u}{\sigma_{\mathrm{s}}^2} \exp\left(-\frac{u^2+\nu_0^2}{2\sigma_{\mathrm{s}}^2}\right) I_0\left(\frac{u\nu_0}{\sigma_{\mathrm{s}}^2}\right), \quad u > 0, \tag{11}$$

where $I_0(\cdot)$ is the modified Bessel function of the first kind with order zero. The PDF of V_0 is:

$$f_{V_0}(\nu_0) = \frac{\nu_0}{\sigma_{\mathrm{u}}^2} \exp\left(-\frac{\nu_0^2}{2\sigma_{\mathrm{u}}^2}\right), \quad \nu_0 > 0. \tag{12}$$

Proof: For the special case of Thomas cluster process, the PDF of $\mathbf{Y}_{\mathrm{s}}$ with realization $\mathbf{y}_{\mathrm{s}} = (y_{\mathrm{s}_1}, y_{\mathrm{s}_2})$ can be expressed as:

$$f_{\mathbf{Y}_s}(y_{\mathrm{s}_1}, y_{\mathrm{s}_2}) = \frac{1}{2\pi\sigma_{\mathrm{s}}^2} \exp\left(-\frac{y_{\mathrm{s}_1}^2 + y_{\mathrm{s}_2}^2}{2\sigma_{\mathrm{s}}^2}\right).$$

Substituting $f_{\mathbf{Y}_s}(\cdot)$ into (8) and letting $z_1 = u\cos\theta$, we get Rician distribution as:

$$f_U(u|\nu_0) = \frac{u}{\sigma_{\mathrm{s}}^2} \exp(-\frac{u^2+\nu_0^2}{2\sigma_{\mathrm{s}}^2}) \underbrace{\int_{-\pi/2}^{\pi_2} \frac{1}{2\pi} \exp(\frac{u\nu_0\cos\theta}{\sigma_{\mathrm{s}}^2})\,\mathrm{d}\theta}_{I_0(\frac{u\nu_0}{\sigma_{\mathrm{s}}^2})},$$

where $F_U(u|\nu_0) = 1 - \int_u^\infty f_U(u|\nu_0)\mathrm{d}u$. Similarly, the PDF of V_0 can be obtained by substituting (1) in (9), which is Rayleigh distribution. ■

The conditional i.i.d. property of distances in the set $\mathcal{D}_{\mathrm{s}}^{\mathbf{x}_0}$ enables us to characterize the distance from the typical user to its nearest open-access SBS located within the representative cluster. This result is presented in the next Lemma.

Lemma 2. *Conditioned on the distance of the typical user to its cluster center, i.e. V_0, the CDF of distance from the typical user to its nearest open-access SBS, i.e., R_{s}, for a given $V_0 = \nu_0$ is:*

$$F_{R_{\mathrm{s}}}(r_{\mathrm{s}}|\nu_0) = 1 - (1 - F_U(r_{\mathrm{s}}|\nu_0))^{n_{\mathrm{s}_0}}, \tag{13}$$

and the conditional PDF of $R_{\rm s}$ for a given ν_0 is:

$$f_{R_{\rm s}}(r_{\rm s}|\nu_0) = n_{{\rm s}_0}(1 - F_U(r_{\rm s}|\nu_0))^{n_{{\rm s}_0}-1} f_U(r_{\rm s}|\nu_0), \tag{14}$$

where $F_U(\cdot|\nu_0)$ and $f_U(\cdot|\nu_0)$ are given by (7) *and* (8)*, respectively.*

Proof: Conditioned on the distance of the typical user to its cluster center, the elements in $\mathcal{D}_{\rm s}^{\mathbf{x}_0}$ are i.i.d. with PDF $f_U(\cdot|\nu_0)$. Thus the result simply follows from the PDF of the minimum element of the i.i.d. sequence of random variables [58, eqn. (3)]. ■

These distance distributions are the keys to the derivation of the metrics of interest.

B. Association policies

As discussed above, the candidate serving BS in each open-access tier (i.e., all macro BSs and SBSs located within the representative cluster) is the one nearest to the user. Recall that the distances from a typical user to its nearest open-access small cell and macro BSs were denoted by $R_{\rm s}$ and $R_{\rm m}$, respectively. In order to select the serving BS from amongst the candidate serving BSs, we consider the following two association policies.

1) Power-based association policy: The serving BS is chosen from amongst the candidate serving BSs according to maximum received-power averaged over small-scale fading. The association event to macro BSs and SBSs can be formally defined as follows.

- A typical user is associated to a macrocell if ${\rm m} = \arg\max_{j\in\{{\rm s},{\rm m}\}} P_j R_j^{-\alpha}$. The association event to macrocell is denoted by $S_{\rm m}^{\rm P}$, where $\mathbf{1}_{S_{\rm m}^{\rm P}} = \mathbf{1}({\rm m} = \arg\max_{j\in\{{\rm s},{\rm m}\}} P_j R_j^{-\alpha})$.
- A typical user is associated to a small cell if ${\rm s} = \arg\max_{j\in\{{\rm s},{\rm m}\}} P_j R_j^{-\alpha}$. The association event to the small cell is denoted by $S_{\rm s}^{\rm P}$, where $\mathbf{1}_{S_{\rm s}^{\rm P}} = \mathbf{1}({\rm s} = \arg\max_{j\in\{{\rm s},{\rm m}\}} P_j R_j^{-\alpha})$.

Now, the density functions of distances $f_{R_{\rm s}}(\cdot|\nu_0)$ and $f_{R_{\rm m}}(\cdot)$ obtained in the previous subsection are used to characterize the association probabilities to macro and small cells in the next Lemma.

Lemma 3 (Association probability under power-based policy)**.** *The association probability of a typical user located at distance ν_0 from its cluster center to macrocell is:*

$$\mathcal{A}_{\rm m}^{\rm P}(\nu_0) = \int_0^\infty \left[1 - F_{R_{\rm s}}\left(\xi_{\rm sm} r_{\rm m}|\nu_0\right)\right] f_{R_{\rm m}}(r_{\rm m}) {\rm d}r_{\rm m}, \tag{15}$$

with $\xi_{\rm sm} = \left(\frac{P_{\rm s}}{P_{\rm m}}\right)^{1/\alpha}$, and the association probability to the small cell is:

$$\mathcal{A}_{\rm s}^{\rm P}(\nu_0) = 1 - \mathcal{A}_{\rm m}^{\rm P}(\nu_0), \tag{16}$$

where $f_{R_{\rm m}}(\cdot)$ and $F_{R_{\rm s}}(\cdot|\nu_0)$ are given by (6) *and* (13)*, respectively.*

Proof: See Appendix B. ■

The serving distance is simply the distance from the typical user to its nearest BS from associated tier. Denote by X_j^{P} the serving distance to tier $j \in \{\mathrm{m}, \mathrm{s}\}$. The density function of X_j^{P} is characterized in the next Lemma.

Lemma 4 (Serving distance distribution under power-based policy)**.** *For a typical user located at distance ν_0 from its cluster center, the PDF of serving distance $X_{\mathrm{m}}^{\mathrm{P}}$ conditioned on the association to macrocell, i.e., event $S_{\mathrm{m}}^{\mathrm{P}}$, is:*

$$f_{X_{\mathrm{m}}^{\mathrm{P}}}(x_{\mathrm{m}}|\nu_0) = \frac{1}{\mathcal{A}_{\mathrm{m}}^{\mathrm{P}}(\nu_0)}(1 - F_{R_{\mathrm{s}}}(\xi_{\mathrm{sm}} x_{\mathrm{m}}|\nu_0)) f_{R_{\mathrm{m}}}(x_{\mathrm{m}}), \text{ and} \tag{17}$$

the PDF of $X_{\mathrm{s}}^{\mathrm{P}}$ conditioned on the association to small cell, i.e., event $S_{\mathrm{s}}^{\mathrm{P}}$, is:

$$f_{X_{\mathrm{s}}^{\mathrm{P}}}(x_{\mathrm{s}}|\nu_0) = \frac{1}{\mathcal{A}_{\mathrm{s}}^{\mathrm{P}}(\nu_0)}(1 - F_{R_{\mathrm{m}}}(\xi_{\mathrm{ms}} x_{\mathrm{s}})) f_{R_{\mathrm{s}}}(x_{\mathrm{s}}|\nu_0), \tag{18}$$

where $\xi_{\mathrm{sm}} = \left(\frac{P_{\mathrm{s}}}{P_{\mathrm{m}}}\right)^{1/\alpha}$ and $\xi_{\mathrm{ms}} = \left(\frac{P_{\mathrm{m}}}{P_{\mathrm{s}}}\right)^{1/\alpha}$. The density functions of distances $f_{R_{\mathrm{m}}}(\cdot)$, $f_{R_{\mathrm{s}}}(\cdot|\nu_0)$, and $F_{R_{\mathrm{s}}}(\cdot|\nu_0)$ are given by (6)*,* (14)*, and* (13)*, respectively.*

Proof: See Appendix C. ■

From power-based association policy, it can be deduced that there are no open-access BSs within distance $\xi_{\mathrm{ms}} x_{\mathrm{s}}$ ($\xi_{\mathrm{sm}} x_{\mathrm{m}}$) of the typical user when this user is served by small cell (macrocell) BS. This can be interpreted as an exclusion zone with radius $\xi_{\mathrm{ms}} x_{\mathrm{s}}$ or $\xi_{\mathrm{sm}} x_{\mathrm{m}}$ depending upon the choice of serving BS, which is centered at the location of the typical user. The effect of exclusion zone on the interference caused by macro BSs (distributed according to a homogeneous PPP Φ_{m}) can be easily handled using Slivnyak's Theorem, which states that the distribution of the PPP conditioned on the location of a point of PPP (here serving BS) is the same as that of the original PPP [56]. However, characterizing the effect of exclusion zone on the distribution of distances from clustered open-access interfering SBSs to the typical user is more challenging. We define the set $\mathcal{F}_{\mathrm{s}}^{\mathrm{P}}(\mathcal{F}_{\mathrm{m}}^{\mathrm{P}})$ to represent the sequence of distances from open access interfering SBSs (which by assumption belong to the representative cluster centered at $\mathbf{x}_0$) to the typical user conditioned on the serving BS belonging to small cell (macrocell), such that the elements of $W_{\mathrm{s}}^{\mathrm{P}} \in \mathcal{F}_{\mathrm{s}}^{\mathrm{P}}$ and $W_{\mathrm{m}}^{\mathrm{P}} \in \mathcal{F}_{\mathrm{m}}^{\mathrm{P}}$ are greater than $\xi_{\mathrm{ms}} x_{\mathrm{s}}$ and $\xi_{\mathrm{sm}} x_{\mathrm{m}}$, respectively. In the next Lemma, we deal with the conditional i.i.d. property of the elements of $\mathcal{F}_{\mathrm{s}}^{\mathrm{P}}$ and $\mathcal{F}_{\mathrm{m}}^{\mathrm{P}}$, and their distributions.

Lemma 5 (Power-based association: distribution of distances from open-access interfering SBSs)**.** *Under power-based association policy, the elements of $\mathcal{F}_{\mathrm{m}}^{P}$ ($\mathcal{F}_{\mathrm{s}}^{P}$) conditioned on V_0 and $X_{\mathrm{m}}^{\mathrm{P}}(X_{\mathrm{s}}^{\mathrm{P}})$*

are i.i.d., where the PDF of each element $W_{\mathrm{m}}^{\mathrm{P}} \in \mathcal{F}_{\mathrm{m}}^{P}$ *for a given* $V_0 = \nu_0$ *and* $X_{\mathrm{m}}^{\mathrm{P}} = x_{\mathrm{m}}$ *is:*

$$f_{W_{\mathrm{m}}^{\mathrm{P}}}(w_{\mathrm{m}}|\nu_0, x_{\mathrm{m}}) = \frac{f_U(w_{\mathrm{m}}|\nu_0)}{1 - F_U(\xi_{\mathrm{sm}} x_{\mathrm{m}}|\nu_0)}, \tag{19}$$

and the conditional PDF of each element $W_{\mathrm{s}}^{\mathrm{P}} \in \mathcal{F}_{\mathrm{s}}^{P}$ *is:*

$$f_{W_{\mathrm{s}}^{\mathrm{P}}}(w_{\mathrm{s}}|\nu_0, x_{\mathrm{s}}) = \frac{f_U(w_{\mathrm{s}}|\nu_0)}{1 - F_U(x_{\mathrm{s}}|\nu_0)}, \tag{20}$$

where $F_U(\cdot|\nu_0)$ *and* $f_U(\cdot|\nu_0)$ *are given by* (7) *and* (8)*, respectively.*

Proof: See Appendix D. ■

2) Distance-based association policy: In addition to received signal strength based association discussed above, it is often times desirable to define simple canonical association policies, which provide useful first order insights into otherwise complicated spatial networks. We define one such association policy next, which we term as *distance-based* association policy. Under this policy, the association event to the SBS and macro Bs is defined as follows.

- A typical user is associated to the small cell if $R_{\mathrm{s}} \leq D$. The association event to the small cell is denoted by $S_{\mathrm{s}}^{\mathrm{D}}$, where $\mathbf{1}_{S_{\mathrm{s}}^{\mathrm{D}}} = \mathbf{1}(R_{\mathrm{s}} \leq D)$.
- A typical user is associated to the macrocell if $R_{\mathrm{s}} > D$. The association event to the macrocell is denoted by $S_{\mathrm{m}}^{\mathrm{D}}$, where $\mathbf{1}_{S_{\mathrm{m}}^{\mathrm{D}}} = \mathbf{1}(R_{\mathrm{s}} > D)$.

Here D denotes the SBS distance threshold. In contrast to the power-based association rule, which is a function of the distances from both the nearest macro and small cell BSs to a typical user, the distance-based association rule is only a function of the distance of a typical user to its nearest open-access SBS, which lends relatively more tractability to the analysis. This simple policy allows us to balance load across macro and small cells by tuning the value of D (where D essentially puts a threshold on the received signal strength from the nearest small cell). The exact impact of D on the coverage probability will be studied in the later sections. In the next Lemma, we characterize the association probabilities to the macro and small cells.

Lemma 6 (Association probability under distance-based policy)**.** *The association probability of a typical user located at distance* ν_0 *from its cluster center to the small cell is:*

$$\mathcal{A}_{\mathrm{s}}^{\mathrm{D}}(\nu_0) = F_{R_{\mathrm{s}}}(D|\nu_0), \tag{21}$$

and the association probability to the macrocell is:

$$\mathcal{A}_{\mathrm{m}}^{\mathrm{D}}(\nu_0) = 1 - \mathcal{A}_{\mathrm{s}}^{\mathrm{D}}(\nu_0), \tag{22}$$

where $F_{R_{\mathrm{s}}}(\cdot|\nu_0)$ *is given by* (13)*.*

Proof: According to the definition of $S_{\rm s}^{\rm D}$, the conditional association probability to the small cell for a given $V_0 = \nu_0$ can be written as: $\mathcal{A}_{\rm s}^{\rm D}(\nu_0) = \mathbb{E}_{R_{\rm s}}[\mathbf{1}(R_{\rm s} < D)|\nu_0] = \mathbb{P}(R_{\rm s} < D|\nu_0) = F_{R_{\rm s}}(D|\nu_0)$, using which the association probability to macrocell is $\mathcal{A}_{\rm m}^{\rm D}(\nu_0) = 1 - F_{R_{\rm s}}(D|\nu_0)$. ■

Using the macro and small cell association probabilities, the density function of serving distance is derived in the next Lemma.

Lemma 7 (Serving distance PDF under distance-based policy)**.** *Under distance-based association policy, the PDF of serving distance $X_{\rm s}^{\rm D}$ when the typical user located at distance ν_0 from its own cluster center is served by a small cell is:*

$$f_{X_{\rm s}^{\rm D}}(x_{\rm s}|\nu_0) = \frac{f_{R_{\rm s}}(x_{\rm s}|\nu_0)}{\mathcal{A}_{\rm s}^{\rm D}(\nu_0)}, \quad 0 \le x_{\rm s} \le D, \tag{23}$$

and the PDF of serving serving distance $X_{\rm s}^{\rm D}$ when the typical user is served by a macrocell is:

$$f_{X_{\rm m}^{\rm D}}(x_{\rm m}) = f_{R_{\rm m}}(x_{\rm m}), \quad x_{\rm m} \ge 0, \tag{24}$$

where $f_{R_{\rm m}}(\cdot)$, $f_{R_{\rm s}}(\cdot|\nu_0)$ and $\mathcal{A}_{\rm s}^{\rm D}(\nu_0)$ are given by (6)*,* (14)*, and* (21)*, respectively.*

Proof: For the typical user located at distance ν_0 from its own cluster center, $f_{X_{\rm s}^{\rm D}}(x_{\rm s}|\nu_0)$ is the PDF of distance from the typical user to its nearest open-access SBS conditioned on the association to small cell tier $S_{\rm s}^{\rm D}$, which is equal to $f_{R_{\rm s}}(x_{\rm s}|S_{\rm s}^{\rm D}, \nu_0)$. However, the association to the macrocell is independent of the distance from the typical user to its nearest macro BS. Thus the PDF of serving distance when the typical user is served by macrocell is simply the PDF of distance to its nearest macro BS. ■

As has already been discussed earlier, the locations of open-access interfering BSs depend upon the association event. From distance-based association policy, it can be deduced that if a typical user is served by small cell (macrocell), the closest open-access interfering SBS must be at distance greater than $x_{\rm s}$ (D) from the typical user. Denote by $\mathcal{F}_{\rm s}^{\rm D}$ ($\mathcal{F}_{\rm m}^{\rm D}$) the sequence of distances from intra-cluster interfering SBSs to the typical user served by small cell (macrocell). The distributions of the elements of $\mathcal{F}_{\rm s}^{\rm D}$ and $\mathcal{F}_{\rm m}^{\rm D}$ are given in the next Lemma.

Lemma 8 (Distance-based association: distribution of distances from open-access interfering SBSs)**.** *Under distance-based association policy, the elements in the sequence of distances from open-access interfering SBSs to the typical user served by macrocell, i.e., $\mathcal{F}_{\rm m}^{D}$, conditioned on V_0 are i.i.d., where the PDF of each element $W_{\rm m}^{\rm D} \in \mathcal{F}_{\rm m}^{D}$ is:*

$$f_{W_{\rm m}^{\rm D}}(w_{\rm m}|\nu_0) = \frac{f_U(w_{\rm m}|\nu_0)}{1 - F_U(D|\nu_0)}, \tag{25}$$

and the elements in the sequence of distances from open-access interfering SBSs to the typical user served by small cell, i.e., $\mathcal{F}_{\rm s}^{D}$, are conditionally i.i.d., where the PDF of each element $W_{\rm s}^{\rm D} \in \mathcal{F}_{\rm m}^{D}$ for given $V_0 = \nu_0$ and $X_{\rm s}^{\rm D} = x_{\rm s}$ is:

$$f_{W_{\rm s}^{\rm D}}(w_{\rm s}|\nu_0, x_{\rm s}) = \frac{f_U(w_{\rm s}|\nu_0)}{1 - F_U(x_{\rm s}|\nu_0)}, \tag{26}$$

where $F_U(\cdot|\nu_0)$ and $f_U(\cdot|\nu_0)$ are given by (7) *and* (8)*, respectively.*

Proof: The proof follows on the same lines as that of Lemma 5, and is hence skipped. ■

The locations of closed-access interfering SBSs are independent of access policy. Thus the distribution of distances from the typical user to the closed-access SBSs (also called inter-cluster interfering SBSs) is the same for both distance-based and power-based association policies. This distribution is presented in the next Lemma.

Lemma 9 (Distribution of distances from closed-access interfering SBSs)**.** *Denote by $\mathcal{D}_{\rm s}^{\mathbf{x}} = \{t_{\rm s} : t_{\rm s} = \|\mathbf{x} + \mathbf{y}_{\rm s}\|, \forall\ \mathbf{y}_{\rm s} \in \mathcal{N}^{\mathbf{x}}\}$ the sequence of distances from the typical user to inter-cluster interfering SBSs within the cluster centered at $\mathbf{x} \in \Psi_{\rm p}$. For a given $v = \|\mathbf{x}\|$, the elements of $\mathcal{D}_{\rm s}^{\mathbf{x}}$ are i.i.d., with PDF*

$$f_{T_{\rm s}}(t_{\rm s}|\nu) = \int_{-t_{\rm s}}^{t_{\rm s}} \frac{t_{\rm s}}{\sqrt{t_{\rm s}^2 - z^2}} \Big[f_{\mathbf{Y}_{\rm s}}\big(z - \nu, \sqrt{t_{\rm s}^2 - z^2}\big) + f_{\mathbf{Y}_{\rm s}}\big(z - \nu, -\sqrt{t_{\rm s}^2 - z^2}\big) \Big] {\rm d}z,\ t_{\rm s} > 0. \tag{27}$$

Proof: The elements of the sequence $\mathcal{N}^{\mathbf{x}}$, i.e., relative locations of the SBSs to the cluster centered at $\mathbf{x} \in \Psi_{\rm p}$, are i.i.d. by assumption. Hence, for a given $\nu = \|\mathbf{x}\|$, the elements of the sequence $\mathcal{D}_{\rm s}^{\mathbf{x}}$ are i.i.d. The derivation of $f_{T_{\rm s}}(\cdot|\nu)$ follows on the same lines as that of $f_U(\cdot|\nu_0)$ given by (8), and hence is skipped. ■

Remark 1 (Thomas cluster process)**.** *For the special case of Thomas cluster process, the elements in the sequence of distances from closed-access interfering SBSs to the typical user are i.i.d., where the PDF of each element is:*

$$f_{T_{\rm s}}(t_{\rm s}|\nu) = \frac{t_{\rm s}}{\sigma_{\rm s}^2} \exp\left(-\frac{t_{\rm s}^2 + \nu^2}{2\sigma_{\rm s}^2}\right) I_0\left(\frac{t_{\rm s}\nu}{\sigma_{\rm s}^2}\right), \quad t_{\rm s} > 0, \tag{28}$$

which is Rician. The proof is exactly the same as that of Corollary 1. It should be noted that all the results can be specialized to Thomas cluster process by substituting $F_U(\cdot|\nu_0)$, $f_U(\cdot|\nu_0)$, $f_{V_0}(\cdot)$, and $f_{T_{\rm s}}(\cdot|\nu)$ with the expressions given by (10)*,* (11)*,* (12)*, and* (28)*, respectively.*

IV. Coverage Probability and throughput Analysis

This is the second main technical section of this paper, where we use the distance distributions and association probabilities derived in the previous section to characterize network performance in terms of coverage probability of a typical user and throughput of the whole network.

A. Coverage probability

The coverage probability can be formally defined as the probability that SIR experienced by a typical user is greater than the desired threshold for successful demodulation and decoding. Mathematically, it is $\mathtt{P_c} = \mathbb{E}[\mathbf{1}(\mathtt{SIR} > \beta)] = \mathbb{P}(\mathtt{SIR} > \beta)$, where β is the target SIR threshold. We specialize this definition to the power-based and the distance-based association policies in this subsection. We begin our discussion with the power-based association.

1) Power-based association policy: As evident in the sequel, the Laplace transform of (the PDF of) interference is the key intermediate result for the coverage probability analysis. Thus we first focus on the derivation of the Laplace transform of interference distribution. As has already been described earlier, the contribution of the total interference seen at a typical user can be partitioned into three sources: i) interference caused by open-access SBSs, ii) interference caused by closed-access SBSs, and iii) interference caused by open-access macro BSs. We now use the distance distributions presented in Lemma 5 to characterize the Laplace transform of interference originating from the open-access SBSs (intra-cluster interferers) in the next Lemma.

Lemma 10. *Under power-based association policy, the conditional Laplace transform of interference distribution caused by open-access SBSs at a typical user served by macrocell, $\mathcal{I}_{\mathrm{sm}}^{\mathrm{intra}}$, for a given $X_{\mathrm{m}}^{\mathrm{P}} = x_{\mathrm{m}}$ and $V_0 = \nu_0$ is:*

$$\mathcal{L}^{\mathrm{P}}_{\mathcal{I}_{\mathrm{sm}}^{\mathrm{intra}}}(s|\nu_0, x_{\mathrm{m}}) = \sum_{\ell=0}^{n_{\mathrm{s}_0}} \left(\int_{\xi_{\mathrm{sm}} x_{\mathrm{m}}}^{\infty} \frac{1}{1 + sP_{\mathrm{s}} w_{\mathrm{m}}^{-\alpha}} f_{W_{\mathrm{m}}^{\mathrm{P}}}(w_{\mathrm{m}}|\nu_0, x_{\mathrm{m}}) \mathrm{d}w_{\mathrm{m}} \right)^{\ell} \frac{\bar{n}_{\mathrm{as}}^{\ell} e^{-\bar{n}_{\mathrm{as}}}}{\ell! \sum_{k=0}^{n_{\mathrm{s}_0}} \frac{\bar{n}_{\mathrm{as}}^{k} e^{-\bar{n}_{\mathrm{as}}}}{k!}}, \tag{29}$$

and the Laplace transform of interference distribution caused by open-access SBSs at a typical user served by small cell, $\mathcal{I}_{\mathrm{ss}}^{\mathrm{intra}}$, is:

$$\mathcal{L}^{\mathrm{P}}_{\mathcal{I}_{\mathrm{ss}}^{\mathrm{intra}}}(s|\nu_0, x_{\mathrm{s}}) = \sum_{\ell=1}^{n_{\mathrm{s}_0}} \left(\int_{x_{\mathrm{s}}}^{\infty} \frac{1}{1 + sP_{\mathrm{s}} w_{\mathrm{s}}^{-\alpha}} f_{W_{\mathrm{s}}^{\mathrm{P}}}(w_{\mathrm{s}}|\nu_0, x_{\mathrm{s}}) \mathrm{d}w_{\mathrm{s}} \right)^{\ell-1} \frac{\bar{n}_{\mathrm{as}}^{\ell} e^{-\bar{n}_{\mathrm{as}}}}{\ell! \sum_{k=1}^{n_{\mathrm{s}_0}} \frac{\bar{n}_{\mathrm{as}}^{k} e^{-\bar{n}_{\mathrm{as}}}}{k!}}, \tag{30}$$

where $f_{W_{\mathrm{m}}^{\mathrm{P}}}(\cdot|\nu_0, x_m)$ and $f_{W_{\mathrm{s}}^{\mathrm{P}}}(\cdot|\nu_0, x_s)$ are given by Lemma 5.

Proof: See Appendix E. ■

Recall that the total number of SBSs in the representative cluster was assumed to be known *a priori* and equal to n_{s_0}. This assumption was made to simplify order statistic argument used in the derivation of the PDF of serving distance, but it constraints the maximum number of interfering SBSs in the representative cluster, which complicates the numerical evaluation of the exact coverage probability (will be presented in Theorem 1) due to the summation involved in the expressions given by Lemma 10. However, these expressions can be simplified under the assumption of $\bar{n}_{\mathrm{as}} \ll n_{s_0}$, and the simplified expressions are presented in the next Corollary.

Corollary 2. *For $\bar{n}_{\mathrm{as}} \ll n_{s_0}$, the Laplace transform of interference given by* (29) *reduces to*

$$\mathcal{L}^{\mathrm{P}}_{\mathcal{I}^{\mathrm{intra}}_{\mathrm{sm}}}(s|\nu_0, x_{\mathrm{m}}) = \exp\Big(\bar{n}_{\mathrm{as}} \int_{\xi_{\mathrm{sm}} x_{\mathrm{m}}}^{\infty} \frac{1}{1+\frac{w_{\mathrm{m}}^{\alpha}}{sP_{\mathrm{s}}}} f_{W^{\mathrm{P}}_{\mathrm{m}}}(w_{\mathrm{m}}|\nu_0)\mathrm{d}w_{\mathrm{m}}\Big), \tag{31}$$

and the Laplace transform of interference given by (30) *reduces to*

$$\mathcal{L}^{\mathrm{P}}_{\mathcal{I}^{\mathrm{intra}}_{\mathrm{ss}}}(s|\nu_0, x_{\mathrm{s}}) = \frac{\exp\Big(\bar{n}_{\mathrm{as}} \int_{x_{\mathrm{s}}}^{\infty} \frac{1}{1+sP_{\mathrm{s}}w_{\mathrm{s}}^{-\alpha}} f_{W^{\mathrm{P}}_{\mathrm{s}}}(w_{\mathrm{s}}|\nu_0, x_{\mathrm{s}})\mathrm{d}w_{\mathrm{s}} - 1\Big)}{(\exp(\bar{n}_{\mathrm{as}}) - 1)\int_{x_{\mathrm{s}}}^{\infty} \frac{1}{1+sP_{\mathrm{s}}w_{\mathrm{s}}^{-\alpha}} f_{W^{\mathrm{P}}_{\mathrm{s}}}(w_{\mathrm{s}}|\nu_0, x_{\mathrm{s}})\mathrm{d}w_{\mathrm{s}}}. \tag{32}$$

For numerical evaluation, we will use the simpler expression presented in Corollary 2 instead of Lemma 10. In the numerical results section, we will notice that the simplified expressions given by Corollary 2 can be treated as a proxy of the exact expression for a wide range of cases.

Using the PDF of distance derived in Lemma 9, we can derive the Laplace transform of interference distribution caused by closed-access interfering SBSs to the typical user (inter-cluster interference), which is stated in the next Lemma.

Lemma 11. *The Laplace transform of interference distribution from closed-access interfering SBSs to the typical user is:*

$$\mathcal{L}_{\mathcal{I}^{\mathrm{inter}}_{\mathrm{s}j}}(s) = \exp\Big(-2\pi\lambda_{\mathrm{p}} \int_0^{\infty} \Big(1 - \exp\Big(-p_{\mathrm{a}}\bar{n}_{\mathrm{s}} \int_0^{\infty} \frac{sP_{\mathrm{s}}{t_{\mathrm{s}}}^{-\alpha}}{1+sP_{\mathrm{s}}{t_{\mathrm{s}}}^{-\alpha}} f_{T_{\mathrm{s}}}(t_{\mathrm{s}}|\nu)\mathrm{d}t_{\mathrm{s}}\Big)\Big)\nu\mathrm{d}\nu\Big), \tag{33}$$

where index $j \in \{m, s\}$ denotes the tier of the serving BS, and $f_{T_{\mathrm{s}}}(\cdot|\nu)$ is given by (27)*.*

Proof: See Appendix F. ■

After dealing with the interference from all open and closed-access SBSs, we now focus on the Laplace transform of interference caused by macro BSs.

Lemma 12. *The Laplace transform of interference from macro BSs (except the serving BS) at the typical user is:*

$$\mathcal{L}^{\mathrm{P}}_{\mathcal{I}_{\mathrm{m}j}}(s) = \exp\Big(-2\pi\lambda_m \int_{\xi_{\mathrm{m}j}x_j}^{\infty} \frac{sP_{\mathrm{m}}u^{-\alpha}}{1+sP_{\mathrm{m}}u^{-\alpha}} u\mathrm{d}u\Big), \tag{34}$$

where index $j \in \{\mathrm{m}, \mathrm{s}\}$ denotes the choice of the serving BS.

Proof: The proof follows from that of [17, Theorem 1] with a minor modification. For completeness, the proof is presented in Appendix G of two column draft. ■

These Laplace transforms of interference distributions are used to evaluate the coverage probability in the next Theorem.

Theorem 1 (Coverage probability under power-based association policy)**.** *Coverage probability of a typical user served by the j^{th} tier is* $\mathtt{P}^{\mathrm{P}}_{\mathrm{c}_j} = \mathbb{E}[\mathbf{1}\{\mathtt{SIR}_j > \beta\}, S^{\mathrm{P}}_j] =$

$$\int_0^\infty \int_0^\infty \mathcal{A}^{\mathrm{P}}_j(\nu_0)\mathcal{L}^{\mathrm{P}}_{\mathcal{I}^{\mathrm{intra}}_{\mathrm{s}j}}\Big(\beta\frac{{x_j}^\alpha}{P_j}|\nu_0, x_j\Big)\mathcal{L}_{\mathcal{I}^{\mathrm{inter}}_{\mathrm{s}j}}\Big(\beta\frac{{x_j}^\alpha}{P_j}\Big)\mathcal{L}^{\mathrm{P}}_{\mathcal{I}_{\mathrm{m}j}}\Big(\beta\frac{{x_j}^\alpha}{P_j}\Big) f_{X^{\mathrm{P}}_j}(x_j|\nu_0) f_{V_0}(\nu_0)\mathrm{d}x_j\mathrm{d}\nu_0, \tag{35}$$

where $j \in \{\mathrm{m}, \mathrm{s}\}$. Using $\mathtt{P}^{\mathrm{P}}_{\mathrm{c}_j}$, the total coverage probability is:

$$\mathtt{P}^{\mathrm{P}}_{\mathrm{c_T}} = \mathtt{P}^{\mathrm{P}}_{\mathrm{c_m}} + \mathtt{P}^{\mathrm{P}}_{\mathrm{c_s}}, \tag{36}$$

where $f_{V_0}(\cdot)$, $\mathcal{A}^{\mathrm{P}}_j(\cdot)$, $f_{X^{\mathrm{P}}_j}(\cdot|\nu_0)$, $\mathcal{L}^{\mathrm{P}}_{\mathcal{I}^{\mathrm{intra}}_{\mathrm{s}j}}(\cdot|\nu_0, x_j)$, $\mathcal{L}_{\mathcal{I}^{\mathrm{inter}}_{\mathrm{s}j}}(\cdot)$, and $\mathcal{L}^{\mathrm{P}}_{\mathcal{I}_{\mathrm{m}j}}(\cdot)$ are given by Lemmas 1, 3, 4, 5, 11, and 12, respectively.

Proof: The coverage probability of a typical user served by the j^{th} tier is:

$$\begin{aligned}\mathtt{P}^{\mathrm{P}}_{\mathrm{c}_j} &= \mathbb{E}\Big[\mathbf{1}\Big\{h_j \geq \beta\frac{{x_j}^\alpha}{P_j}(\mathcal{I}_{\mathrm{m}j} + \mathcal{I}^{\mathrm{intra}}_{\mathrm{s}j} + \mathcal{I}^{\mathrm{inter}}_{\mathrm{s}j})\Big\}\Big] \\ &\overset{(a)}{=} \mathbb{E}_{V_0}\Big[\mathbb{E}_{X^{\mathrm{P}}_j}\Big[\mathbb{E}\Big[\exp\Big(-\beta\frac{{x_j}^\alpha}{P_j}(\mathcal{I}_{\mathrm{m}j} + \mathcal{I}^{\mathrm{intra}}_{\mathrm{s}j} + \mathcal{I}^{\mathrm{inter}}_{\mathrm{s}j})\Big)|X^{\mathrm{P}}_j\Big]\Big]\mathbb{E}\Big[S^{\mathrm{P}}_j\Big]|V_0\Big],\end{aligned}$$

where (a) follows from Rayleigh fading assumption, i.e., $h_j \sim \exp(1)$, and the fact that the events $\mathbf{1}\{\mathtt{SIR}_j > \beta\}$ and S^{P}_j conditioned on V_0 are independent. Recall that the association probabilities are given by Lemma 3. The final expression of $\mathtt{P}^{\mathrm{P}}_{\mathrm{c}_j}$ given by (35) is obtained by using the definition of Laplace transform along with independence of open-access (intra-cluster), closed-access (inter-cluster) SBSs, and macro BSs interference powers, followed by de-conditioning over X^{P}_j given $V_0 = \nu_0$, followed by de-conditioning over V_0. Now using $\mathtt{P}^{\mathrm{P}}_{\mathrm{c}_j}$, the total coverage probability is obtained by applying the law of total probability. ■

2) Distance-based association policy: We now extend the coverage probability analysis to the case where the serving BS is chosen according to the distance based association policy. Similar to the previous subsection, we begin by deriving the Laplace transform of interference distribution. Using the PDF of distance derived in Lemma 8, the Laplace transform of interference caused by open-access interfering SBSs is characterized in the next Lemma.

Lemma 13. *Under distance-based association policy, the Laplace transform of interference caused by open-access SBSs at a typical user served by macrocell, $\mathcal{I}_{\mathrm{sm}}^{\mathrm{intra}}$, conditioned on V_0 is:*

$$\mathcal{L}^{\mathrm{D}}_{\mathcal{I}_{\mathrm{sm}}^{\mathrm{intra}}}(s|\nu_0) = \sum_{\ell=0}^{n_{\mathrm{s}_0}} \left(\int_D^{\infty} \frac{1}{1+sP_{\mathrm{s}}w_{\mathrm{m}}^{-\alpha}} f_{W_{\mathrm{m}}^{\mathrm{D}}}(w_{\mathrm{m}}|\nu_0)\mathrm{d}w_{\mathrm{m}} \right)^{\ell} \frac{\bar{n}_{\mathrm{as}}^{\ell} e^{-\bar{n}_{\mathrm{as}}}}{\ell! \sum_{k=0}^{n_{\mathrm{s}_0}} \frac{\bar{n}_{\mathrm{as}}^{k} e^{-\bar{n}_{\mathrm{as}}}}{k!}}, \tag{37}$$

which for $\bar{n}_{\mathrm{as}} \ll n_{s_0}$ simplifies to

$$\mathcal{L}^{\mathrm{D}}_{\mathcal{I}_{\mathrm{sm}}^{\mathrm{intra}}}(s|\nu_0) = \exp\left(\bar{n}_{\mathrm{as}} \int_D^{\infty} \frac{1}{1+\frac{w_{\mathrm{m}}^{\alpha}}{sP_{\mathrm{s}}}} f_{W_{\mathrm{m}}^{\mathrm{D}}}(w_{\mathrm{m}}|\nu_0)\mathrm{d}w_{\mathrm{m}} \right), \tag{38}$$

where $f_{W_{\mathrm{m}}^{\mathrm{D}}}(\cdot|\nu_0)$ is given by (25)*. The Laplace transform of interference caused by open-access SBSs at a typical small cell user under distance-based association policy is the same as that of power-based association policy. Thus we have $\mathcal{L}^{\mathrm{D}}_{\mathcal{I}_{\mathrm{ss}}^{\mathrm{intra}}}(s|\nu_0, x_{\mathrm{s}}) = \mathcal{L}^{\mathrm{P}}_{\mathcal{I}_{\mathrm{ss}}^{\mathrm{intra}}}(s|\nu_0, x_{\mathrm{s}})$.*

Proof: The proof follows on the same lines as that of Lemma 10, where the nearest open-access SBS is located at distance greater than D to the typical user served by macrocell. ■

As noted above, the interference caused by closed-access SBSs is independent of association policy, and hence its Laplace transform is the same for the two association policies. Now we are left with the derivation of the Laplace transform of interference caused by macro BSs, which is presented in the next Lemma.

Lemma 14. *The Laplace transform of interference from macro BSs at a typical user served by small cell is:*

$$\mathcal{L}^{\mathrm{D}}_{\mathcal{I}_{\mathrm{ms}}}(s) = \exp\left(-\pi\lambda_{\mathrm{m}} \frac{(sP_{\mathrm{m}})^{\frac{2}{\alpha}}}{\mathrm{sinc}(\frac{2}{\alpha})} \right), \tag{39}$$

and the Laplace transform of interference from macro BSs (except serving) at a typical user served by macrocell under distance-based association policy is the same as that of the power-based association policy. Thus we have $\mathcal{L}^{\mathrm{D}}_{\mathcal{I}_{\mathrm{mm}}}(s) = \mathcal{L}^{\mathrm{P}}_{\mathcal{I}_{\mathrm{mm}}}(s)$.

Proof: The proof follows on the same lines as that of Lemma 12. The main difference is that the distance-based association policy imposes no constraint on the location of interfering macro BSs to the typical user served by the small cell. Thus we have

$$\mathcal{L}^{\mathrm{D}}_{\mathcal{I}_{\mathrm{ms}}}(s) = \exp\Big(-2\pi\lambda_m \int_0^{\infty} \frac{sP_{\mathrm{m}}u^{-\alpha}}{1+sP_{\mathrm{m}}u^{-\alpha}} u\mathrm{d}u \Big),$$

where the final expression is obtained by using [59, (3.241)]. ■

Using these Lemmas, we now derive the coverage probability of a typical user under distance based association policy. The proof follows on the same lines as that of Theorem 1.

Theorem 2 (Coverage probability under distance-based association policy)**.** *The coverage probability of a typical user served by small cell is:* $\mathtt{P}_{\mathrm{c_s}}^{\mathrm{D}} = \mathbb{E}[\mathbf{1}\{\mathtt{SIR}_{\mathrm{s}} > \beta\}, S_{\mathrm{s}}^{\mathrm{D}}] =$

$$\int_0^{\infty}\int_0^{D} \mathcal{A}_{\mathrm{s}}^{\mathrm{D}}(\nu_0)\mathcal{L}_{\mathcal{I}_{\mathrm{ss}}^{\mathrm{intra}}}^{\mathrm{D}}(\beta\frac{{x_{\mathrm{s}}}^{\alpha}}{P_{\mathrm{s}}}|\nu_0, x_{\mathrm{s}})\mathcal{L}_{\mathcal{I}_{\mathrm{ss}}^{\mathrm{inter}}}(\beta\frac{{x_{\mathrm{s}}}^{\alpha}}{P_{\mathrm{s}}})\mathcal{L}_{\mathcal{I}_{\mathrm{ms}}}^{\mathrm{D}}(\beta\frac{{x_{\mathrm{s}}}^{\alpha}}{P_{\mathrm{s}}})f_{X_{\mathrm{s}}^{\mathrm{D}}}(x_{\mathrm{s}}|\nu_0)f_{V_0}(\nu_0)\mathrm{d}x_{\mathrm{s}}\mathrm{d}\nu_0, \quad (40)$$

and the coverage probability of a typical user served by macrocell is:

$$\mathtt{P}_{\mathrm{c_m}}^{\mathrm{D}} = \mathbb{E}[\mathbf{1}\{\mathtt{SIR}_{\mathrm{m}} > \beta\}, S_{\mathrm{m}}^{\mathrm{D}}] = \int_0^{\infty}\int_0^{\infty} \mathcal{A}_{\mathrm{m}}^{\mathrm{D}}(\nu_0)\mathcal{L}_{\mathcal{I}_{\mathrm{sm}}^{\mathrm{intra}}}^{\mathrm{D}}(\beta\frac{{x_{\mathrm{m}}}^{\alpha}}{P_{\mathrm{m}}}|\nu_0)\mathcal{L}_{\mathcal{I}_{\mathrm{sm}}^{\mathrm{inter}}}(\beta\frac{{x_{\mathrm{m}}}^{\alpha}}{P_{\mathrm{m}}})$$
$$\times \mathcal{L}_{\mathcal{I}_{\mathrm{mm}}}^{\mathrm{D}}(\beta\frac{{x_{\mathrm{m}}}^{\alpha}}{P_{\mathrm{m}}})f_{X_{\mathrm{m}}^{\mathrm{D}}}(x_{\mathrm{m}})f_{V_0}(\nu_0)\mathrm{d}x_{\mathrm{m}}\mathrm{d}\nu_0, \quad (41)$$

using which the total coverage probability is:

$$\mathtt{P}_{\mathrm{c_T}}^{\mathrm{D}} = \mathtt{P}_{\mathrm{c_m}}^{\mathrm{D}} + \mathtt{P}_{\mathrm{c_s}}^{\mathrm{D}}, \quad (42)$$

where $f_{V_0}(\cdot)$*,* $\mathcal{A}_j^{\mathrm{D}}(\cdot)$*,* $f_{X_j^{\mathrm{D}}}(\cdot)$*,* $\mathcal{L}_{\mathcal{I}_{\mathrm{sj}}^{\mathrm{intra}}}^{\mathrm{D}}(\cdot)$*,* $\mathcal{L}_{\mathcal{I}_{\mathrm{sj}}^{\mathrm{inter}}}(\cdot)$*, and* $\mathcal{L}_{\mathcal{I}_{\mathrm{mm}}}^{\mathrm{D}}(\cdot)$ *are given by Lemmas 1, 6, 7, 13, 11, and 14, respectively.*

Remark 2 (Optimal SBS distance threshold D)**.** *Increasing SBS distance threshold has a conflicting effect on the association to macrocell and small cell: association probability to macrocell decreases whereas association probability to small cell increases. In the Numerical Results Section, we concretely demonstrate that there exists an optimal SBS distance threshold* D *that maximizes the total coverage probability.*

Using these coverage probability results, we now characterize throughput in the next subsection.

B. Throughput

In order to study the tradeoff between aggressive frequency reuse and resulting interference, we use the following notion of the network *throughput* [28]:

$$\mathcal{T} = \lambda \log_2(1+\beta)\mathtt{P_c}, \quad (43)$$

where λ is the number of simultaneously active transmitters per unit area. This metric roughly characterizes the average number of bits successfully transmitted per unit area. This definition is specialized to our setup in the next Proposition.

Proposition 1. *Using the result of Theorem 1, the throughput under power-based association policy is:*

$$\mathcal{T}^{\mathrm{P}} = (\lambda_{\mathrm{m}}\mathtt{P}_{\mathrm{c_m}}^{\mathrm{P}} + \lambda_{\mathrm{p}}\bar{n}_{\mathrm{as}}\mathtt{P}_{\mathrm{c_s}}^{\mathrm{P}})\log_2(1+\beta), \quad (44)$$

and using the result of Theorem 2, the throughput under distance-based association policy is:

$$\mathcal{T}^{\mathrm{D}} = (\lambda_{\mathrm{m}}\mathtt{P}^{\mathrm{D}}_{\mathrm{c_m}} + \lambda_{\mathrm{p}}\bar{n}_{\mathrm{as}}\mathtt{P}^{\mathrm{D}}_{\mathrm{c_s}})\log_2(1+\beta). \tag{45}$$

Remark 3 (Number of simultaneously active SBSs within a cluster)**.** *Increasing number of simultaneously active SBSs boosts the spectral efficiency by more aggressive frequency reuse, whilst it leads to higher interference power. While it is straightforward to conclude from the analytical results that the coverage probability always decreases with the number of simultaneously active SBSs, we will demonstrate in the next section that the throughput increases with the number of simultaneously active SBSs in the regime of interest. This in turn implies that the usual assumption of strictly orthogonal channelization per cluster, i.e., only one simultaneously active SBSs per cluster (e.g., see [47]), should be revisited.*

V. Results and Discussion

A. Validation of results

In this section, we validate the accuracy of the analysis by comparing the analytical results with Monte Carlo simulations. For this comparison, the macro BS locations are distributed as an independent PPP with density $\lambda_{\mathrm{m}} = 1$ km^{-2}, and the geographical centers of user hotspots (i.e., cluster centers) are distributed as an independent PPP with density $\lambda_{\mathrm{p}} = 10$ km^{-2} around which users and SBSs are assumed to be normally distributed with variances σ^2_{u} and σ^2_{s}, respectively. For this setup, we set the path-loss exponent, α as 4, the SIR threshold as 0 dB, power ratio $P_{\mathrm{m}} = 10^3 P_{\mathrm{s}}$, and study the coverage probability for the two association policies. As discussed in Section IV, the summation involved in the exact expression of Laplace transform of intra-cluster interference complicates the numerical evaluation of Theorems 1 and 2. Thus we use simpler expressions of Laplace transform of intra-cluster interference derived under the assumption $\bar{n}_{\mathrm{as}} \ll n_{s_0}$ presented in Corollary 2 and Lemma 13 for numerical evaluation of Theorems 1 and 2. As evident from Figs. 2 and 3, the simpler expressions can be treated as proxies of exact for wide range of parameters. Considering $n_{s_0} = 10$, the analytical plots exhibit perfect match with simulation even for relatively large values of $\bar{n}_{\mathrm{as}}$. Comparing Figs 2 and 3, we also note that the coverage probability under power-based association policy is higher than that of distance-based association policy.

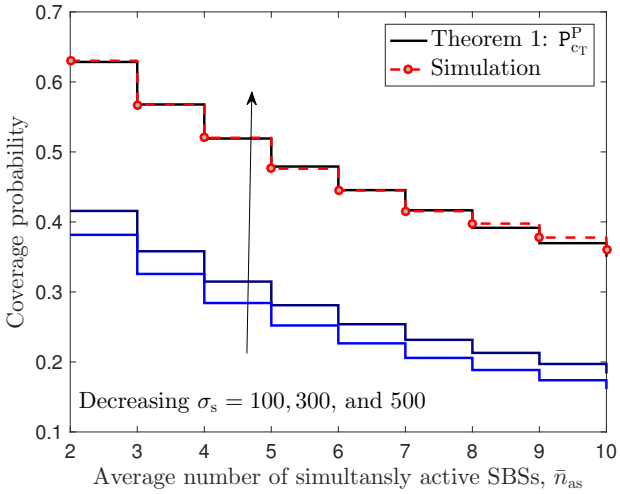
Theorem 1: $\mathrm{P}_{\mathrm{cT}}^{\mathrm{P}}$
Simulation
Coverage probability
Decreasing $\sigma_{\mathrm{s}} = 100, 300$, and 500
Average number of simultansly active SBSs, $\bar{n}_{\mathrm{as}}$

Fig. 2. Coverage probability as a function of averaged number of simultaneously active SBSs for different value of σ_{s} under power-based association policy ($n_{s_0} = 10$ and $\sigma_{\mathrm{s}} = \sigma_{\mathrm{u}}$)

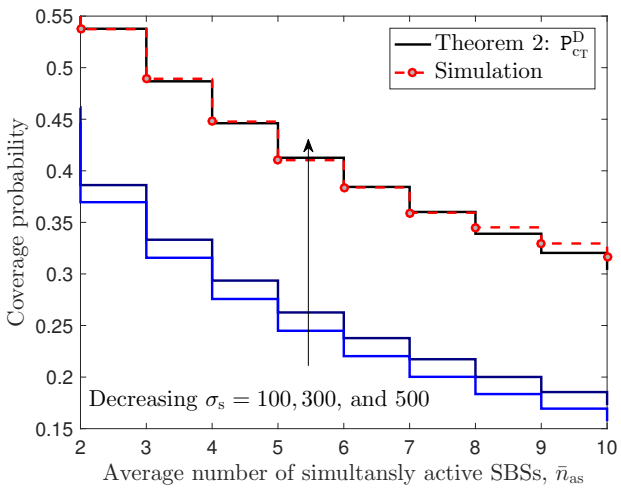
Theorem 2: $\mathrm{P}_{\mathrm{cT}}^{\mathrm{D}}$
Simulation
Coverage probability
Decreasing $\sigma_{\mathrm{s}} = 100, 300$, and 500
Average number of simultansly active SBSs, $\bar{n}_{\mathrm{as}}$

Fig. 3. Coverage probability as a function of averaged number of simultaneously active SBSs for different value of σ_{s} under distance-based association policy ($n_{s_0} = 10$ and $\sigma_{\mathrm{s}} = \sigma_{\mathrm{u}}$)

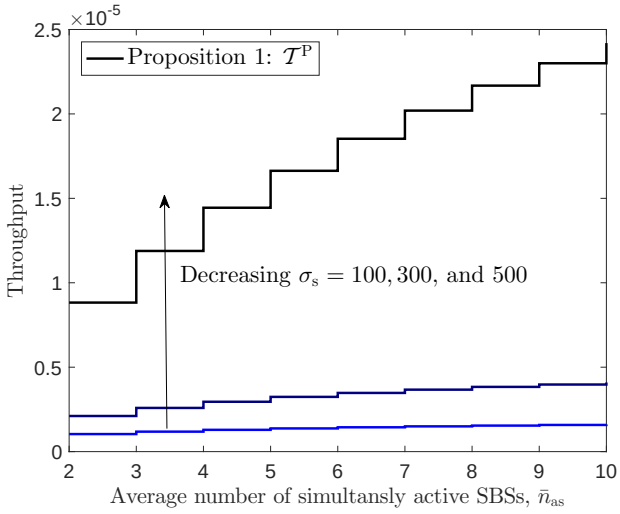
$\times 10^{-5}$
Proposition 1: $\mathcal{T}^{\mathrm{P}}$
Throughput
Decreasing $\sigma_{\mathrm{s}} = 100, 300$, and 500
Average number of simultansly active SBSs, $\bar{n}_{\mathrm{as}}$

Fig. 4. Throughput as a function of averaged number of simultaneously active SBSs for different value of σ_{s} under power-based association policy ($n_{s_0} = 10$ and $\sigma_{\mathrm{s}} = \sigma_{\mathrm{u}}$)

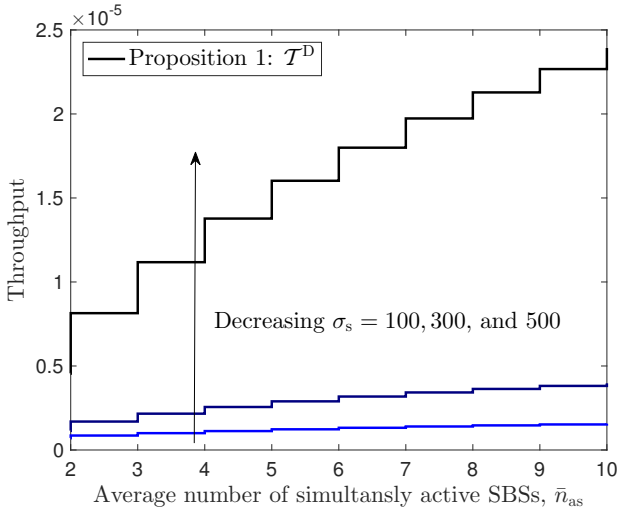
$\times 10^{-5}$
Proposition 1: $\mathcal{T}^{\mathrm{D}}$
Throughput
Decreasing $\sigma_{\mathrm{s}} = 100, 300$, and 500
Average number of simultansly active SBSs, $\bar{n}_{\mathrm{as}}$

Fig. 5. Throughput as a function of averaged number of simultaneously active SBSs for different value of σ_{s} under distance-based association policy ($n_{s_0} = 10$ and $\sigma_{\mathrm{s}} = \sigma_{\mathrm{u}}$)

B. Number of simultaneously active SBSs

The coverage probability as a function of averaged number of simultaneously active SBSs, $\bar{n}_{\mathrm{as}}$, are presented in Figs. 2 and 3 for power-based and distance-based association policies, respectively. Our analysis concretely demonstrates that the coverage probability always decreases when more SBSs per cluster reuse the same spectrum. This is because more simultaneously active SBSs results in more interference. However, there is a classical trade-off between frequency reuse

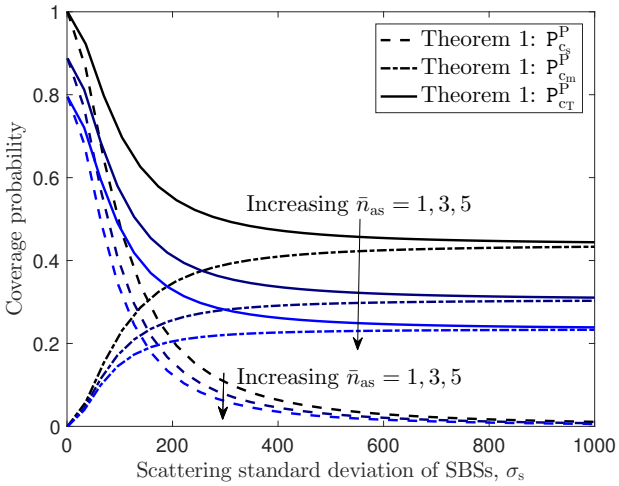

Fig. 6. Coverage probability as a function of standard deviation σ_{s} for different value of $\bar{n}_{\mathrm{as}}$ ($n_{s_0} = 10$ and $\sigma_{\mathrm{s}} = \sigma_{\mathrm{u}}$)

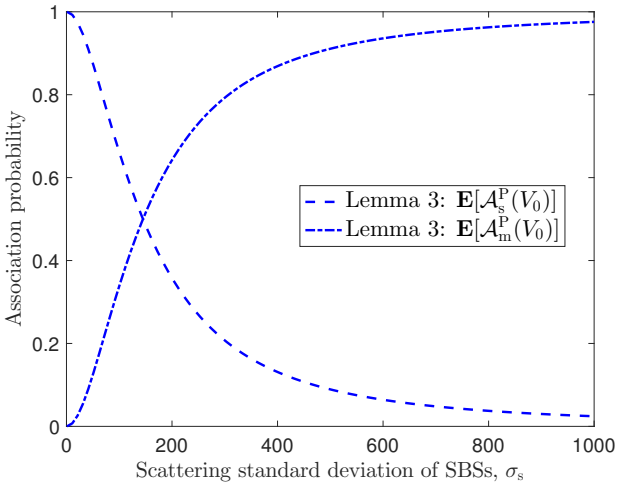

Fig. 7. Association probability as a function of standard deviation σ_{s} ($n_{s_0} = 10$ and $\sigma_{\mathrm{s}} = \sigma_{\mathrm{u}}$)

and resulting interference. To study this trade-off, we plot throughput as a function of $\bar{n}_{\mathrm{as}}$ in Figs. 4 and 5. Interestingly in the considered range, throughput increases with the averaged number of simultaneously active SBSs per cluster. This means that more and more SBSs can be simultaneously activated as long as the coverage probability remains acceptable. From this observation, it can also be deduced that strictly orthogonal strategy (only one SBS per cluster reuses the same resource block) is not spectrally efficient.

C. Impact of SBS standard deviation

Under power-based association policy, the coverage probability as a function of scattering standard deviation of SBSs, σ_{s}, is plotted in Fig. 6. The plot shows that σ_{s} has a conflicting effect on $\mathtt{P}^{\mathrm{P}}_{\mathrm{c_m}}$ and $\mathtt{P}^{\mathrm{P}}_{\mathrm{c_s}}$: $\mathtt{P}^{\mathrm{P}}_{\mathrm{c_m}}$ increases and $\mathtt{P}^{\mathrm{P}}_{\mathrm{c_s}}$ decreases. The intuition behind this observation is that by increasing σ_{s} the association to macrocell increases while association to small cell decreases. In Fig. 7, we plot average association probability as a function of σ_{s} to exhibit this trend. From Fig. 9, a similar observation can be made for distance-based association policy, where $\mathtt{P}^{\mathrm{D}}_{\mathrm{c_m}}$ increases and $\mathtt{P}^{\mathrm{D}}_{\mathrm{c_s}}$ decreases as scattering standard deviation of SBSs increases.

D. Optimal distance threshold

As evident from Figs. 8 and 9, there exists an optimal SBS distance threshold that maximizes the total coverage probability. The existence of the optimal value can be intuitively justified by the conflicting effect of the distance threshold on the association to macrocell and small cell, as

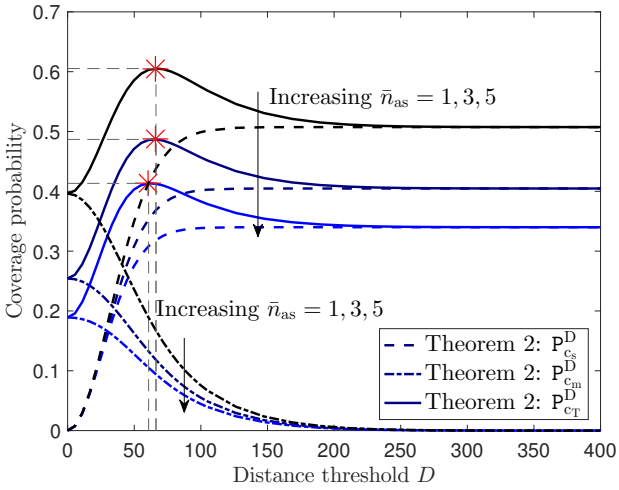
Coverage probability
Distance threshold D
Increasing $\bar{n}_{\rm as} = 1, 3, 5$
Increasing $\bar{n}_{\rm as} = 1, 3, 5$
Theorem 2: $\mathrm{P}^{\mathrm{D}}_{\mathrm{c_s}}$
Theorem 2: $\mathrm{P}^{\mathrm{D}}_{\mathrm{c_m}}$
Theorem 2: $\mathrm{P}^{\mathrm{D}}_{\mathrm{c_T}}$

Fig. 8. Association probability as a function of distance threshold D for different value of $\bar{n}_{\rm as}$ ($n_{s_0} = 10$ and $\sigma_{\rm s} = \sigma_{\rm u}$)

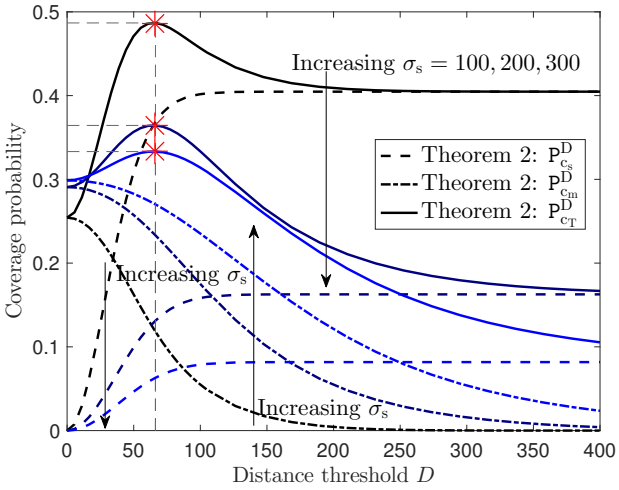

Fig. 9. Coverage probability as a function of distance threshold D for different value of $\sigma_{\rm s}$ ($n_{s_0} = 10$ and $\sigma_{\rm s} = \sigma_{\rm u}$).

discussed in Remark 3. From Fig. 8, we can observe that the optimal distance threshold decreases with the increase of averaged number of simultaneously active SBSs. This is because although both $\mathrm{P}^{\mathrm{D}}_{\mathrm{c_s}}$ and $\mathrm{P}^{\mathrm{D}}_{\mathrm{c_m}}$ decrease with the increase of $\bar{n}_{\rm as}$, the former decreases at a slightly higher rate. Thus it is desired to associate less users to SBSs. Interestingly, we notice that the optimal distance threshold for different values of $\sigma_{\rm s}$ does not change in the setup considered in Fig. 9.

VI. Concluding Remarks

We developed a comprehensive framework for the performance analysis of HetNets with user-centric capacity-driven small cell deployments. Unlike the prior art on the spatial modeling of HetNets where users and SBSs are usually modeled by independent homogeneous PPPs, we introduced a tractable approach to incorporate correlation in the locations of the users and SBSs in HetNets, which bridges the gap between the simulation models used by industry (especially for the use hotspots), such as by 3GPP [2], and the ones used thus far by the stochastic geometry community. In particular, we assumed that the geographical centers of user hotspots are distributed according to a homogeneous PPP around which users and SBSs are located with two general distributions. This approach not only models the aforementioned correlation, but also captures the non-homogeneous nature of user distributions [2]. For this setup, we derived the coverage probability of a typical user and throughput of the whole network for distance-based and power-based association policies. Our setup is general and applicable to any distributions of the relative locations of the users and SBSs with respect to the cluster center. A key intermediate

step is the derivation of a new set of distance distributions, which enabled the accurate analysis of user-centric small deployments. For numerical evaluation, we considered the special case of Thomas cluster process, which led to several design insights. The most important one is that the throughput increases with the increase of the number of SBSs per cluster reusing the same resource block in the considered setup. Therefore, the usual assumption of strictly orthogonal channelization per cluster should be revisited for efficient design, planning, and dimensioning of the system.

This work has many extensions. From modeling perspective, it is important to extend the analysis to more general channel models, such as $\kappa - \mu$ shadowed fading channels [60], and correlated shadowing [61]. From analysis perspective, it is useful to study the connection between simplified protocol and physical layer interference models to gain more system design insights from analytical expressions. From application perspective, the results can be extended to the analysis of cache enabled network to study metrics like total hit probability and caching throughput; see [48], [62]. From point process perspective, it is of interest to jointly model the spatial separation between the locations of macro BSs and SBSs as well as clustering nature of SBSs, which brings forth a new set of challenges in the context of cluster point processes [63]. Finally, this framework can be extended to the analysis of other key performance metrics such as ergodic spectral efficiency [64] and bit error rate.

APPENDIX

A. *Proof of Lemma 1*

Let us denote the location of SBS chosen uniformly at random in the representative cluster by $\mathbf{z}_0 = \mathbf{x}_0 + \mathbf{y}_\mathrm{s} \in \mathbb{R}^2$, where $\mathbf{z}_0 = (z_1, z_2)$ and $\mathbf{x}_0 = (\nu_0, 0)$. The conditional CDF of distance U with realization $u = \sqrt{z_1^2 + z_2^2} \in \mathbb{R}_+$ is:

$$F_U(u|\mathbf{x}_0) = F_U(u|\nu_0) = \int\int_{\sqrt{z_1^2+z_2^2}\leq u} f_{\mathbf{Y}_\mathrm{s}}\big(z_1 - \nu_0, z_2\big)\mathrm{d}z_2\mathrm{d}z_1$$
$$= \int_{z_1=-u}^{z_1=u}\int_{z_2=-\sqrt{u^2-z_1^2}}^{z_2=\sqrt{u^2-z_1^2}} f_{\mathbf{Y}_\mathrm{s}}\big(z_1 - \nu_0, z_2\big)\mathrm{d}z_2\mathrm{d}z_1,$$

where the PDF of U is obtained by using Leibniz's rule for differentiation [65]. Now recall that the typical user is located at the origin, and users are distributed around cluster center with PDF $f_{\mathbf{Y}_\mathrm{u}}(\mathbf{y_u})$. Thus, the relative location of the cluster center with respect to the typical user, i.e x_0,

has the same distribution as that of $\mathbf{Y}_{\rm u}$. The PDF of $V_0 = \|\mathbf{Y}_u\|$ can be derived by using the same argument applied in the derivation of $f_U(.)$.

B. Proof of Lemma 3

The conditional association probability to the macro-tier for a given value of ν_0 is:

$$\mathcal{A}^{\rm P}_{\rm m}(\nu_0) = \mathbb{E}_{R_{\rm m}}[\mathbf{1}\{P_{\rm m}R_{\rm m}^{-\alpha} > P_{\rm s}R_{\rm s}^{-\alpha}\}|\nu_0] = \int_0^\infty \mathbb{P}\Big[R_{\rm s} > \big(\frac{P_{\rm s}}{P_{\rm m}}\big)^{1/\alpha} r_{\rm m}|\nu_0\Big] f_{R_{\rm m}}(r_{\rm m}){\rm d}r_{\rm m},$$
$$= \int_0^\infty \Big[1 - F_{R_{\rm s}}\big(\big(\frac{P_{\rm s}}{P_{\rm m}}\big)^{1/\alpha} r_{\rm m}|\nu_0\big)\Big] f_{R_{\rm m}}(r_{\rm m}){\rm d}r_{\rm m},$$

using which the association probability to the small cell tier is $\mathcal{A}^{\rm P}_{\rm s}(\nu_0) = 1 - \mathcal{A}^{\rm P}_{\rm m}(\nu_0)$.

C. Proof of Lemma 4

For a given typical user located at distance ν_0 from its cluster center, the event $X^{\rm P}_{\rm m} > x_{\rm m}$ is equivalent to that of $R_{\rm m} > x_{\rm m}$ when the typical user connects to the macro BS, i.e., event $S^{\rm P}_{\rm m}$. Thus, the conditional CCDF of $X^{\rm P}_{\rm m}$ can be derived as:

$$\mathbb{P}(X^{\rm P}_{\rm m} > x_{\rm m}|\nu_0) = \mathbb{P}(R_{\rm m} > x_{\rm m}|S^{\rm P}_{\rm m}, \nu_0) = \frac{\mathbb{P}[R_{\rm m} > x_{\rm m}, S^{\rm P}_{\rm m}|\nu_0]}{\mathbb{P}[S^{\rm P}_{\rm m}|\nu_0]} \tag{46}$$

$$= \frac{1}{\mathcal{A}^{\rm P}_{\rm m}(\nu_0)} \int_{x_{\rm m}}^\infty \mathbb{P}(R_{\rm s} > \xi_{\rm sm}\, r_{\rm m}|\nu_0) f_{R_{\rm m}}(r_{\rm m}){\rm d}r_{\rm m}, \tag{47}$$

and hence the PDF of $X^{\rm P}_{\rm m}$ is:

$$f_{X^{\rm P}_{\rm m}}(x_{\rm m}|\nu_0) = \frac{\rm d}{{\rm d}x_{\rm m}}(1 - \mathbb{P}(X^{\rm P}_{\rm m} > x_{\rm m}|\nu_0)) = \frac{1}{\mathcal{A}^{\rm P}_{\rm m}(\nu_0)}(1 - F_{R_{\rm s}}(\xi_{\rm sm}x_{\rm m}|\nu_0)) f_{R_{\rm m}}(x_{\rm m}). \tag{48}$$

The derivation of $f_{X^{\rm P}_{\rm s}}(\cdot|\nu_0)$ follows on the same lines as that of $f_{X^{\rm P}_{\rm m}}(\cdot|\nu_0)$, and is hence skipped.

D. Proof of Lemma 5

Denote by $\{U_j\}_{j=1}^{n_{\rm s_0}}$ the sequence of distances from open access SBSs to the typical user. From power-based association policy, it can be deduced that there are no open-access BSs within distance $\xi_{\rm sm}x_{\rm m}$ if the typical user is served by macro BS. Thus, the sequence of distances from interfering open-access SBSs to the typical user can be defined as $\mathcal{F}^{\rm P}_{\rm m} \equiv \{W^{\rm P}_{{\rm m},j} : W^{\rm P}_{{\rm m},j} = U_j, U_j > \xi_{\rm sm}x_{\rm m}\}$. The conditional joint density function of the elements in $\mathcal{F}^{\rm P}_{\rm m}$ is:

$$\mathbb{P}(W^{\rm P}_{{\rm m},1} < w_{{\rm m},1}, ..., W^{\rm P}_{{\rm m},n_{\rm s_0}} < w_{{\rm m},n_{\rm s_0}}|V_0 = \nu_0)$$
$$= \mathbb{P}(U_1 < w_{{\rm m},1}, ..., U_{n_{\rm s_0}} < w_{{\rm m},n_{\rm s_0}}|U_1 > \xi_{\rm sm}x_{\rm m}, ..., U_{n_{\rm s}} > \xi_{\rm sm}x_{\rm m}, V_0 = \nu_0)$$
$$= \begin{cases} \frac{\mathbb{P}(U_1 < w_{{\rm m},1}, ..., U_{n_{\rm s_0}} < w_{{\rm m},n_{\rm s_0}}|V_0 = \nu_0)}{\mathbb{P}(U_1 > \xi_{\rm sm}x_{\rm m}, ..., U_{n_{\rm s}} > \xi_{\rm sm}x_{\rm m}|V_0 = \nu_0)}, & w_{{\rm m},j} \geq \xi_{\rm sm}x_{\rm m} \\ 0, & 0 \leq w_{{\rm m},j} < \xi_{\rm sm}x_{\rm m} \end{cases}, \quad j = \{1, 2, ..., n_{\rm s_0}\}$$

$$\overset{(a)}{=}\begin{cases}\prod_{j=1}^{n_{\mathrm{s}_0}}\frac{F_{U_j}(w_{\mathrm{m},j}|\nu_0)}{1-F_{U_j}(\xi_{\mathrm{sm}}x_{\mathrm{m}}|\nu_0)}, & w_{\mathrm{m},j}\geq\xi_{\mathrm{sm}}x_{\mathrm{m}}\\ 0, & 0\leq w_{\mathrm{m},j}<\xi_{\mathrm{sm}}x_{\mathrm{m}}\end{cases}, \quad j=\{1,2,...,n_{\mathrm{s}_0}\},$$

where (a) follows from the fact that the elements in $\{U_j\}_{j=1}^{n_{\mathrm{s}_0}}$ are conditionally i.i.d. (see Lemma 1). The product of the same functional form in the joint CDF implies that the elements in $\mathcal{F}_{\mathrm{m}}^{\mathrm{P}}$ are conditionally i.i.d. with CDF $F_{W_{\mathrm{m},j}^{\mathrm{P}}}(w_{\mathrm{m},j}|\nu_0,x_{\mathrm{m}})=\frac{F_{U_j}(w_{\mathrm{m},j}|\nu_0)}{1-F_{U_j}(\xi_{\mathrm{sm}}x_{\mathrm{m}}|\nu_0)}$. Using this result, the PDF of $W_{\mathrm{m},j}^{\mathrm{P}}$ can be obtained by taking derivative of $F_{W_{\mathrm{m},j}^{\mathrm{P}}}(w_{\mathrm{m},j}|\nu_0,x_{\mathrm{m}})$ with respect to $w_{\mathrm{m},j}$. In the final result, index j is dropped for notational simplicity. The derivation of $f_{W_{\mathrm{s}}^{\mathrm{P}}}(\cdot|\nu_0,x_{\mathrm{s}})$ follows on the same line as that of $W_{\mathrm{m}}^{\mathrm{P}}$, and is hence skipped.

E. Proof of Lemma 10

The Laplace transform of intra-cluster interference distribution at a typical user served by macrocell conditioned on V_0 and $X_{\mathrm{m}}^{\mathrm{P}}$ is:

$$\mathcal{L}_{\mathcal{I}_{\mathrm{sm}}^{\mathrm{intra}}}(s|\nu_0,x_{\mathrm{m}})\overset{(a)}{=}\mathbb{E}\Big[\exp\Big(-s\sum_{\mathbf{y}_{\mathrm{s}}\in\mathcal{B}_{\mathrm{s}}^{\mathbf{x}_0}}P_{\mathrm{s}}h_{\mathrm{s}}\|\mathbf{x}_0+\mathbf{y}_{\mathrm{s}}\|^{-\alpha}\Big)\Big]\overset{(b)}{=}\mathbb{E}\Big[\prod_{\mathbf{y}_{\mathrm{s}}\in\mathcal{B}_{\mathrm{s}}^{\mathbf{x}_0}}\frac{1}{1+sP_{\mathrm{s}}\|\mathbf{x}_0+\mathbf{y}_{\mathrm{s}}\|^{-\alpha}}\Big],$$

where (a) follows from the definition of Laplace transform, (b) follows from the expectation over $h_{\mathrm{s}}\sim\exp(1)$. The final result follows from the change of variable $\|\mathbf{x}_0+\mathbf{y}_{\mathrm{s}}\|\to w_{\mathrm{m}}$, and converting coordinates from Cartesian to polar, followed by the fact that the elements of $\{W_{\mathrm{m}}\}$ are conditionally i.i.d., with PDF $f_{W_{\mathrm{m}}^{\mathrm{P}}}(w_{\mathrm{m}}|\nu_0,x_{\mathrm{m}})$ given by Lemma 5, followed by the expectation over number of simultaneously active SBSs within the representative cluster, which is Poisson distributed conditioned on the total being less than n_{s_0}. The derivation of $\mathcal{L}_{\mathcal{I}_{\mathrm{ss}}^{\mathrm{intra}}}(.|\nu_0,x_{\mathrm{s}})$ follows on the same line as that of $\mathcal{L}_{\mathcal{I}_{\mathrm{sm}}^{\mathrm{intra}}}(.|\nu_0,x_{\mathrm{m}})$, where the serving SBS is removed from the set of possible interfering SBSs, and number of simultaneously active SBSs within the representative cluster is Poisson distributed conditioned on the total being greater than one and less than n_{s_0}.

F. Proof of Lemma 11

Note that the Laplace transform of inter-cluster interference does not depend on the choice of the serving BS. Denoting by $j\in\{\mathrm{s},\mathrm{m}\}$ the index of the serving BS, the Laplace transform of inter-cluster interference $\mathcal{I}_{\mathrm{s}j}^{\mathrm{inter}}$ is $\mathcal{L}_{\mathcal{I}_{\mathrm{s}j}^{\mathrm{inter}}}(s)$

$$\overset{(a)}{=}\mathbb{E}\Big[\exp\Big(-s\sum_{\mathbf{x}\in\Psi_{\mathrm{p}}\setminus\mathbf{x}_0}\sum_{\mathbf{y}_{\mathrm{s}}\in\mathcal{B}_{\mathrm{s}}^{\mathbf{x}}}P_{\mathrm{s}}h_{\mathrm{s}}\|\mathbf{x}+\mathbf{y}_{\mathrm{s}}\|^{-\alpha}\Big)\Big]$$

$$\overset{(b)}{=}\mathbb{E}_{\Psi_{\mathrm{p}}}\prod_{\mathbf{x}\in\Psi_{\mathrm{p}}\setminus\mathbf{x}_0}\mathbb{E}_{\mathcal{B}_{\mathrm{s}}^{\mathbf{x}}}\prod_{\mathbf{y}_{\mathrm{s}}\in\mathcal{B}_{\mathrm{s}}^{\mathbf{x}}}\mathbb{E}_{h_{\mathrm{s}}}\exp\Big(-sP_{\mathrm{s}}h_{\mathrm{s}}\|\mathbf{x}+\mathbf{y}_{\mathrm{s}}\|^{-\alpha}\Big)$$

$$\stackrel{(c)}{=} \mathbb{E}_{\Psi_{\rm p}} \prod_{\mathbf{x}\in\Psi_{\rm p}\setminus\mathbf{x}_0} \mathbb{E}_{\mathcal{B}_{\rm s}^{\mathbf{x}}} \prod_{\mathbf{y}_{\rm s}\in\mathcal{B}_{\rm s}^{\mathbf{x}}} \frac{1}{1+sP_{\rm s}\|\mathbf{x}+\mathbf{y}_{\rm s}\|^{-\alpha}}$$

$$\stackrel{(d)}{=} \mathbb{E}_{\Psi_{\rm p}} \prod_{\mathbf{x}\in\Psi_{\rm p}\setminus\mathbf{x}_0} \exp\Big(-\bar{n}_{\rm as}\int_0^\infty \frac{sP_{\rm s}t_{\rm s}^{-\alpha}}{1+sP_{\rm s}t_{\rm s}^{-\alpha}} f_{T_{\rm s}}(t_{\rm s}|\nu){\rm d}t_{\rm s}\Big)$$

$$\stackrel{(e)}{=} \exp\Big(-2\pi\lambda_{\rm p}\int_0^\infty \Big(1-\exp\Big(-\bar{n}_{\rm as}\int_0^\infty \frac{sP_{\rm s}t_{\rm s}^{-\alpha}}{1+sP_{\rm s}t_{\rm s}^{-\alpha}} f_{T_{\rm s}}(t_{\rm s}|\nu){\rm d}t_{\rm s}\Big)\Big)\nu{\rm d}\nu\Big),$$

where (a) follows from definition of Laplace transform, (b) follow from the assumption that fading gains across all interfering links are independent, (c) follows from the expectation over $h_{\rm s}\sim\exp(1)$, (d) follows from the change of variable $\|\mathbf{x}_0+\mathbf{y}_{\rm s}\|\to t_{\rm s}$, and converting coordinates from Cartesian to polar, followed by the fact that number of points are Poisson distributed, and (e) follows from probability generating functional (PGFL) of PPP.

G. Proof of Lemma 12

Recall that there is no interfering macro BSs within distance $\xi_{{\rm m}j}x_j$ (where $j\in\{{\rm m},{\rm s}\}$ denotes tier of the serving BSs) from the typical user located at the origin. Thus, the points process of interfering macro BSs can be defined as $\Phi'_{\rm m}=\Phi_{\rm m}\setminus\mathbf{b}(\mathbf{o},\xi_{{\rm m}j}x_j)$, where $\mathbf{b}(\mathbf{o},\xi_{{\rm m}j}x_j)$ denotes ball of radius $\xi_{{\rm m}j}x_j$ centered at the origin, i.e., the location of the typical user. The Laplace transform of interference from macro BSs to the typical user is:

$$\mathcal{L}_{\mathcal{I}_{{\rm m}j}}(s) = \mathbb{E}\Big[\exp\Big(-s\sum_{\mathbf{z}_{\rm m}\in\Phi'_m} P_{\rm m}h_{\rm m}\|\mathbf{z}_{\rm m}\|^{-\alpha}\Big)\Big]$$

$$= \mathbb{E}\Big[\prod_{\mathbf{z}_{\rm m}\in\Phi'_{\rm m}} \exp(-sP_{\rm m}h_{\rm m}\|\mathbf{z}_{\rm m}\|^{-\alpha})\Big]$$

$$\stackrel{(a)}{=} \mathbb{E}\Big[\prod_{\mathbf{z}_{\rm m}\in\Phi'_{\rm m}} \frac{1}{1+sP_{\rm m}\|\mathbf{z}_{\rm m}\|^{-\alpha}}\Big]$$

$$\stackrel{(b)}{=} \exp\Big(-2\pi\lambda_m\int_{\xi_{{\rm m}j}x_j}^\infty \frac{su^{-\alpha}}{1+su^{-\alpha}}u{\rm d}u\Big),$$

where (a) follows form expectation over $h_{\rm m}\sim\exp(1)$ and (b) follows from $\|\mathbf{z}_{\rm m}\|\to u$, and converting coordinates from Cartesian to polar, followed by PGFL of PPP.

REFERENCES

[1] M. Afshang and H. S. Dhillon, "A new clustered HetNet model to accurately characterize user-centric small cell deployments," in *Proc. IEEE WCNC*, Oct. 2016.

[2] 3GPP TR 36.814, "Further advancements for E-UTRA physical layer aspects," Tech. Rep., 2010.

[3] 3GPP, "Consideration of UE Cluster Position and PeNB TX Power in Heterogeneous Deployment Configuration 4," Discussion/ Decision R1-100477, Jan. 2010, 8.2.1 Relevant scenarios of Heterogeneous Networks.

[4] V. Chandrasekhar, J. G. Andrews, and A. Gatherer, "Femtocell networks: a survey," *IEEE Commun. Magazine*, vol. 46, no. 9, pp. 59–67, Sep. 2008.

[5] A. Damnjanovic, J. Montojo, Y. Wei, T. Ji, T. Luo, M. Vajapeyam, T. Yoo, O. Song, and D. Malladi, "A survey on 3GPP heterogeneous networks," *IEEE Wireless Commun. Magazine*, vol. 18, no. 3, pp. 10–21, Jun. 2011.

[6] J. G. Andrews, "Seven ways that HetNets are a cellular paradigm shift," *IEEE Commun. Magazine*, vol. 51, no. 3, pp. 136–144, Mar. 2013.

[7] M. Mirahsan, R. Schoenen, and H. Yanikomeroglu, "HetHetNets: Heterogeneous traffic distribution in heterogeneous wireless cellular networks," *IEEE Journal on Sel. Areas in Commun.*, vol. 33, no. 10, pp. 2252–2265, Oct. 2015.

[8] S. Mukherjee, *Analytical Modeling of Heterogeneous Cellular Networks*. Cambridge University Press, 2014.

[9] H. Elsawy, E. Hossain, and M. Haenggi, "Stochastic geometry for modeling, analysis, and design of multi-tier and cognitive cellular wireless networks: A survey," *IEEE Commun. Surveys and Tutorials*, vol. 15, no. 3, pp. 996–1019, 3th quarter 2013.

[10] J. G. Andrews, A. K. Gupta, and H. S. Dhillon, "A primer on cellular network analysis using stochastic geometry," *arXiv preprint*, 2016, available online: arxiv.org/abs/1604.03183.

[11] H. ElSawy, A. Sultan-Salem, M. S. Alouini, and M. Z. Win, "Modeling and analysis of cellular networks using stochastic geometry: A tutorial," *arXiv preprint*, 2016, available online: arxiv.org/abs/1604.03689.

[12] H. S. Dhillon, R. K. Ganti, F. Baccelli, and J. G. Andrews, "Modeling and analysis of K-tier downlink heterogeneous cellular networks," *IEEE Journal on Sel. Areas in Commun.*, vol. 30, no. 3, pp. 550–560, Apr. 2012.

[13] H. S. Dhillon, R. K. Ganti, and J. G. Andrews, "A tractable framework for coverage and outage in heterogeneous cellular networks," in *Information Theory and Applications Workshop (ITA)*, Feb. 2011, pp. 1–6.

[14] J. G. Andrews, F. Baccelli, and R. K. Ganti, "A tractable approach to coverage and rate in cellular networks," *IEEE Trans. on Commun.*, vol. 59, no. 11, pp. 3122–3134, Nov. 2011.

[15] M. D. Renzo and W. Lu, "Stochastic geometry modeling and performance evaluation of MIMO cellular networks using the equivalent-in-distribution (EiD)-based approach," *IEEE Trans. on Commun.*, vol. 63, no. 3, pp. 977–996, Mar. 2015.

[16] S. Mukherjee, "Distribution of downlink SINR in heterogeneous cellular networks," *IEEE Journal on Sel. Areas in Commun.*, vol. 30, no. 3, pp. 575–585, Apr. 2012.

[17] H.-S. Jo, Y. J. Sang, P. Xia, and J. G. Andrews, "Heterogeneous cellular networks with flexible cell association: A comprehensive downlink SINR analysis," *IEEE Trans. on Wireless Commun.*, vol. 11, no. 10, pp. 3484–3495, Oct. 2012.

[18] P. Madhusudhanan, J. G. Restrepo, Y. Liu, T. X. Brown, and K. R. Baker, "Downlink performance analysis for a generalized shotgun cellular system," *IEEE Trans. on Wireless Commun.*, vol. 13, no. 12, pp. 6684–6696, Dec. 2014.

[19] R. Tanbourgi, S. Singh, J. G. Andrews, and F. K. Jondral, "A tractable model for noncoherent joint-transmission base station cooperation," *IEEE Transactions on Wireless Communications*, vol. 13, no. 9, pp. 4959–4973, Sep. 2014.

[20] G. Nigam, P. Minero, and M. Haenggi, "Coordinated multipoint joint transmission in heterogeneous networks," *IEEE Trans. on Commun.*, vol. 62, no. 11, pp. 4134–4146, Nov. 2014.

[21] A. H. Sakr and E. Hossain, "Location-aware cross-tier coordinated multipoint transmission in two-tier cellular networks," *IEEE Transactions on Wireless Communications*, vol. 13, no. 11, pp. 6311–6325, Nov. 2014.

[22] R. W. Heath, M. Kountouris, and T. Bai, "Modeling heterogeneous network interference using poisson point processes," *IEEE Trans. on Signal Processing*, vol. 61, no. 16, pp. 4114–4126, Aug. 2013.

[23] S. Singh, H. S. Dhillon, and J. G. Andrews, "Offloading in heterogeneous networks: Modeling, analysis, and design insights," *IEEE Trans. on Wireless Commun.*, vol. 12, no. 5, pp. 2484–2497, May. 2013.

[24] H. S. Dhillon and J. G. Andrews, "Downlink rate distribution in heterogeneous cellular networks under generalized cell selection," *IEEE Wireless Commun. Letters*, vol. 3, no. 1, pp. 42–45, Feb. 2014.

[25] A. K. Gupta, H. S. Dhillon, S. Vishwanath, and J. G. Andrews, "Downlink multi-antenna heterogeneous cellular network with load balancing," *IEEE Trans. on Commun.*, vol. 62, no. 11, pp. 4052–4067, Nov. 2014.

[26] Y. S. Soh, T. Q. S. Quek, M. Kountouris, and H. Shin, "Energy efficient heterogeneous cellular networks," *IEEE Journal on Sel. Areas in Commun.*, vol. 31, no. 5, pp. 840–850, May 2013.

[27] M. D. Renzo, A. Guidotti, and G. E. Corazza, "Average rate of downlink heterogeneous cellular networks over generalized fading channels: A stochastic geometry approach," *IEEE Trans. on Commun.*, vol. 61, no. 7, pp. 3050–3071, Jul. 2013.

[28] W. C. Cheung, T. Q. S. Quek, and M. Kountouris, "Throughput optimization, spectrum allocation, and access control in two-tier femtocell networks," *IEEE Journal on Sel. Areas in Commun.*, vol. 30, no. 3, pp. 561–574, Apr. 2012.

[29] H. S. Dhillon, Y. Li, P. Nuggehalli, Z. Pi, and J. G. Andrews, "Fundamentals of heterogeneous cellular networks with energy harvesting," *IEEE Trans. on Wireless Commun.*, vol. 13, no. 5, pp. 2782–2797, May. 2014.

[30] H. S. Dhillon, M. Kountouris, and J. G. Andrews, "Downlink MIMO HetNets: Modeling, ordering results and performance analysis," *IEEE Trans. on Wireless Commun.*, vol. 12, no. 10, pp. 5208–5222, Oct. 2013.

[31] C. Li, J. Zhang, and K. B. Letaief, "Throughput and energy efficiency analysis of small cell networks with multi-antenna base stations," *IEEE Trans. on Wireless Commun.*, vol. 13, no. 5, pp. 2505–2517, May 2014.

[32] C. Li, J. Zhang, J. G. Andrews, and K. B. Letaief, "Success probability and area spectral efficiency in multiuser MIMO HetNets," *IEEE Trans. on Commun.*, vol. 64, no. 4, pp. 1544–1556, Apr. 2016.

[33] M. D. Renzo and P. Guan, "A mathematical framework to the computation of the error probability of downlink MIMO cellular networks by using stochastic geometry," *IEEE Trans. on Commun.*, vol. 62, no. 8, pp. 2860–2879, Aug. 2014.

[34] F. Baccelli and A. Giovanidis, "A stochastic geometry framework for analyzing pairwise-cooperative cellular networks," *IEEE Trans. on Wireless Commun.*, vol. 14, no. 2, pp. 794–808, Feb. 2015.

[35] H. S. Dhillon, R. K. Ganti, and J. G. Andrews, "Modeling non-uniform UE distributions in downlink cellular networks," *IEEE Wireless Commun. Letters*, vol. 2, no. 3, pp. 339–342, Jun. 2013.

[36] M. Afshang, H. S. Dhillon, and P. H. J. Chong, "Modeling and performance analysis of clustered device-to-device networks," *IEEE Trans. on Wireless Commun.*, vol. 15, no. 7, pp. 4957–4972, Jul. 2016.

[37] ——, "Fundamentals of cluster-centric content placement in cache-enabled device-to-device networks," *IEEE Trans. on Commun.*, vol. 64, no. 6, pp. 2511–2526, Jun. 2016.

[38] M. Afshang and H. S. Dhillon, "Fundamentals of modeling finite wireless networks using binomial point process," submitted to be *IEEE Trans. on Wireless Commun.*, 2016.

[39] M. Afshang, C. Saha, and H. S. Dhillon, "Nearest-neighbor and contact distance distributions for thomas cluster process," *IEEE Wireless Commun. Letters*, 2016, to appear.

[40] C. Saha and H. S. Dhillon, "Downlink coverage probability of K-tier HetNets with general non-uniformuser distributions," in *Proc., IEEE Intl. Conf. on Commun. (ICC)*, May 2016.

[41] C. Saha, M. Afshang, and H. S. Dhillon, "Enriched K-tier HetNet model to enable the analysis of user-centric small cell deployments," submitted to *IEEE Trans. on Wireless Commun.*, 2016, available online:arxiv.org/abs/1606.06223.

[42] H.Tabassum, E. Hossain, and M. J. Hossain, "Modeling and analysis of uplink non-orthogonal multiple access (NOMA) in large-scale cellular networks using poisson cluster processes," Nov. 2016, available online: arxiv.org/abs/1610.06995.

[43] P. D. Mankar, G. Das, and S. S. Pathak, "Modeling and coverage analysis of BS-centric clustered users in a random wireless network," *IEEE Wireless Commun. Letters*, vol. 5, no. 2, pp. 208–211, Apr. 2016.

[44] J. G. Andrews, R. K. Ganti, M. Haenggi, N. Jindal, and S. Weber, "A primer on spatial modeling and analysis in wireless networks," *IEEE Commun. Magazine*, vol. 48, no. 11, pp. 156–163, Nov. 2010.

[45] C.-H. Lee, C.-Y. Shih, and Y.-S. Chen, "Stochastic geometry based models for modeling cellular networks in urban areas," *Wireless networks*, vol. 19, no. 6, pp. 1063–1072, Oct 2013.

[46] Y. Zhong and W. Zhang, "Multi-channel hybrid access femtocells: A stochastic geometric analysis," *IEEE Trans. on Commun.*, vol. 61, no. 7, pp. 3016–3026, Jul. 2013.

[47] Y. J. Chun, M. O. Hasna, and A. Ghrayeb, "Modeling heterogeneous cellular networks interference using poisson cluster processes," *IEEE Journal on Sel. Areas in Commun.*, vol. 33, no. 10, pp. 2182–2195, Oct. 2015.

[48] E. Baştuğ, M. Bennis, M. Kountouris, and M. Debbah, "Edge caching for coverage and capacity-aided heterogeneous networks," in *Proc., IEEE International Symposium on Information Theory (ISIT)*, Jul. 2016, available online: arxiv.org/abs/1605.00319.

[49] Y. Wang and Q. Zhu, "Modeling and analysis of small cells based on clustered stochastic geometry," *IEEE Commun. Letters*, 2016, to appear.

[50] V. Suryaprakash, J. Møller, and G. Fettweis, "On the modeling and analysis of heterogeneous radio access networks using a poisson cluster process," *IEEE Trans. on Wireless Commun.*, vol. 14, no. 2, pp. 1035–1047, Feb. 2015.

[51] C. Chen, R. C. Elliott, and W. A. Krzymien, "Downlink coverage analysis of n-tier heterogeneous cellular networks based on clustered stochastic geometry," in *Proc., IEEE Asilomar*, Nov. 2013, pp. 1577–1581.

[52] P. D. Mankar, G. Das, and S. Pathak, "Coverage analysis of two-tier HetNets for Co-channel, orthogonal, and partial spectrum sharing under fractional load conditions," Submitted to *IEEE Trans. on Vehicular Technology*, Sep., available online: arxiv.org/abs/1609.05656.

[53] N. Deng, W. Zhou, and M. Haenggi, "Heterogeneous cellular network models with dependence," *IEEE Journal on Selected Areas in Communications*, vol. 33, no. 10, pp. 2167–2181, Oct. 2015.

[54] D. J. Daley and D. Vere-Jones, *An Introduction to the Theory of Point Processes. Volume I: Elementary Theory and Methods*, 2nd ed. New York: Springer-Verlag, 2003.

[55] R. K. Ganti and M. Haenggi, "Interference and outage in clustered wireless ad hoc networks," *IEEE Trans. on Info. Theory*, vol. 55, no. 9, pp. 4067–4086, Sep. 2009.

[56] M. Haenggi, *Stochastic Geometry for Wireless Networks*. Cambridge University Press, 2012.

[57] ——, "On distances in uniformly random networks," *IEEE Trans. on Info. Theory*, vol. 51, no. 10, pp. 3584–3586, Oct. 2005.

[58] H. A. David and H. N. Nagaraja, *Order Statistics*. New York: John Wiley and Sons, 1970.

[59] D. Zwillinger, *Table of integrals, series, and products*. Elsevier, 2014.

[60] Y. J. Chun, S. L. Cotton, H. S. Dhillon, F. J. Lopez-Martinez, J. F. Paris, and S. K. Yoo, "A comprehensive analysis of 5G heterogeneous cellular systems operating over κ-μ shadowed fading channels," submitted to *IEEE Trans. on Wireless Commun.*, Oct. 2016.

[61] N. Ross and D. Schuhmacher, "Wireless network signals with moderately correlated shadowing still appear poisson," *IEEE Trans. on Info. Theory*, 2016, to appear.

[62] M. Afshang and H. S. Dhillon, "Optimal geographic caching in finite wireless networks," in *Proc., IEEE SPAWC*, Jul. 2016, available online: arxiv.org/abs/1603.01921.

[63] ——, "Spatial modeling of device-to-device networks: Poisson cluster process meets Poisson hole process," in *Proc. Asilomar*, Pacific Grove, CA, Nov. 2015.

[64] G. George, R. K. Mungara, A. Lozano, and M. Haenggi, "Ergodic spectral efficiency in mimo cellular networks," submitted to *IEEE Trans. on Wireless Commun.*, Jul. 2016, available online: arxiv.org/abs/1607.04352.

[65] S. G. Samko, A. A. Kilbas, and O. I. Marichev, *Fractional integrals and derivatives: Theory and Applications*. London: Gordon and Breach, 1993.